Engineering Science and Military Technologies
Volume (7) - Issue (2) - Sep 2023
ISSN: 2357- 0954
DOI:10.21608/EJMTC.2023.195782.1249

On the review of magnetic properties of metamaterials CRLH microwave couplers: Design and analysis

Review Article

Mahmoud A. Abdalla[1] and Zihrun Hu[2]

[1]Department of Electronic Engineering, Military Technical College, Cairo, Egypt.
[2]AMACG, EEE School, University of Manchester, UK

Keywords:
Couplers, CRLH transmission lines, ferrite, microwave components.

Corresponding Author:
Mahmoud A. Abdalla, Department of Electronic Engineering, Military Technical College, Cairo, Egypt, **Tel: 0**1118750114, **Email:** maaabdalla@ieee.org

Abstract
This paper introduces a review of the design and analysis of different designs for tunable/nonreciprocal and compact-size microwave couplers. The presented couplers are designed based on composite right/left-handed (CRLH) transmission lines and in the planar structures made of ferrite substrates. The CRLH transmission lines have many attractive features of nonlinearity operation with the frequency that can help the designers to present a compact and different frequency functionality of the presented devices. Moreover, the ferrite substrates are anisotropic media that help the designer to introduce nonreciprocal devices. Mixing the design aspects from CRLH transmission lines and the ferrite substrates can lead to novel properties. According to this approach, we present a collecting review for many microwave couplers with small size/ different frequency functionalities and different tunable/ non-reciprocity properties. The reviewed designs are implemented in coplanar waveguides hosting planar structures that help for reducing the needed DC magnetic bias for the ferrite substrates for its operation. All the reviewed couplers are presented in a detailed explanation of theory parts and complete circuit model and electromagnetic simulations and finally experimental measurements.

I. INTRODUCTION

The great interest in using composite right/left-handed metamaterials-based microwave circuit applications encourages the use of planar composite right/left-handed (CRLH) transmission lines (TLs) versions. CRLH TLs have been realized using transmission lines loaded with either SRR/wire pair[1], CSRR/capacitive gap pairs[2-5], or series capacitive load and shunt inductive load periodically[6-8]. The versions making use of SRR are sometimes called resonant configurations while the others are called non-resonant configurations. The realization of planar non-resonant CRLH TLs is possible in either 1-D TL structure in which the propagation is only along the structure principle's axis[6,7,9,10] or 2-D TL structure which represents all directions of propagations in the 2-D structure[9,11,12-15]. Different configurations of non-resonant 1-D CRLH TLs in either microstrip[9,16,17] or CPW[18-23] configurations have been proposed using different types of loading capacitors and inductors. These studies have included the implementation of series capacitive load through the use of either lumped element capacitor, air gap capacitor, or interdigital capacitor. The shunt inductive load is implemented through the use of a shunt stub inductor or meandered line inductor. Based on these novel transmission lines, several microwave components have been reported in the literature such as couplers, power dividers, filters, and antennas[24-42].

Planar ferrite TL has a dispersive permeability whose value can be negative or positive. It demonstrates evanescent propagation within the frequency band of negative permeability. Also, such propagation can be nonreciprocal depending on the applied DC magnetic bias direction. Therefore, a tunable and nonreciprocal CRLH TL can be expected by using ferrite substrates. However, the ferrite coplanar waveguide (CPW) transmission line has many advantages such as it compatible with MMIC circuits and it needs a small DC biasing magnetic field as a consequence of its small demagnetization factor. Examples of many non-reciprocal CPW couplers, isolators, and circulators are presented in[43-45].

Mixing the features of CRLH TLs and the ferrite substrates have encouraged researchers over years to contribute novel microwave components. Such features have been demonstrated by Tsutsumi[46,47] using microstrip TLs over mixed ferrite and dielectric substrate and by Abdalla[48,49] by using CPW ferrite substrates. Applying these TL configurations, many other reviewers

have presented tunable microwave devices such as resonators[50,51], impedance transformers[52,53], phase shifters[54,55], diplexers[56], isolators[57], circulators[58], leaky wave antennas[59-63] and couplers[64-69] were suggested.

Coupler is a main microwave component that is can be utilized in many microwave circuit applications. Development of microwave communication systems requires enhancement of coupler performances along with a broad bandwidth and compact size. The conventional coupled line coupler consists of two-quarter wave parallel lines, mainly on microstrip. The design of different types of conventional microwave couplers has a trade-off between bandwidth, coupling level, and structure implementation constraints. A coupled line coupler (CLC) has broad bandwidth, of more than 25%, but its coupling level is relatively low. Branch line or rat-race couplers are a 3 dB coupling level, but it has a narrow bandwidth, of less than 10%. The Lange coupler can provide both broad bandwidth and high coupling level, but it has the disadvantage of being limited in operations at lower frequencies due to the introduced parasitic effects at high frequencies due to its bonding wires structure[70-72].

Conventional CLC can be considered a simple coupler type. Its two main disadvantages can be explained as follow. First, it requires very narrow spacing between the parallel lines to achieve a high coupling level of up to 3 dB; otherwise, its coupling level is very low. Second, increasing its forward coupling level requires increasing the electrical length of the two individual TLs[9]. In conventional RH TL, the propagation constant is directly proportional to the frequency and hence the guided wavelength is inversely proportional to the frequency. Thus, with frequency increase, the electric length increases increasing the forward coupling level. Thus, the conventional CLC has a low forward coupling level at a lower frequency at a fixed physical length. In other words, conventional forward CLC needs a very long physical length to achieve a high forward coupling level[9].

The novel properties of the CRLH TL can lead to the novel performance of CRLH CLC[9]. CRLH CLC has overcome the disadvantages of the conventional CLC as follows. First, due to its backward wave propagation, it can demonstrate an arbitrarily high backward coupling level, even 0 dB, over a broad bandwidth, more than 35%, with relatively wide line separation. Second, its two parallel lines have propagation constants inversely proportional to the frequency, and hence guided wavelength is directly proportional to the frequency. Thus, with the frequency decrease, the electric length increases increasing the forward coupling. Therefore, CRLH CLC can demonstrate a high forward coupling level at a lower frequency with shorter lengths compared to conventional ones[73]. Different CRLH CLCs types have been introduced in microstrip[72,74], and CPW[75] configurations.

Tunability and nonreciprocity are unique properties of ferrite medium. It can demonstrate dispersive nature according to the applied DC magnetic bias. In addition to these novel properties, all these microwave components have the advantage of their compact size, being CRLH elements. Also, they require low DC magnetic bias since they have been realized in horizontally magnetization ferrite CPW configuration. Accordingly, by combining the tunable and nonreciprocal characteristics of CRLH TL implemented using ferrite substrate along with the advantages of designing CLCs in CRLH configuration, novel CRLH ferrite CLCs can be introduced. These new couplers will have novel circuit performance which cannot be achieved using either conventional dielectric CRLH CLC or conventional RH ferrite couplers. Promising examples of such ferrite CRLH CLC have been introduced in microstrip configuration[76-78].

In this paper, we review different ferrite CRLH CLC types. These types comprise a tunable almost 0 dB backward CLC with nonreciprocal dual-mode[66,68], a tunable power division backward CLC[66,79], and a nonreciprocal forward CLC[67]. All of the proposed types were designed in CPW configuration and using different CRLH loading elements configurations. Through our review in this paper, we explain the CRLH CLC operation using the generalized coupled mode approach[80]. Then, we explain the performance of the ferrite CRLH CLC by modifying the aforementioned approach, employing ferrite as a substrate. We proceed forward to introduce the different reported couplers starting with ferrite CRLH backward CLCs and following with ferrite CRLH forward CLC. The generalized coupled mode of a general CRLH forward CLC has been developed here for the first time. The performances of each reported coupler type are explained theoretically, verified numerically, and confirmed by experimental measurements. The theoretical analytical studies for the different proposed coupler types are based on the modified generalized ferrite CRLH coupled mode concepts. The numerical studies for all the coupler's performance were done using full-wave electromagnetic simulations. The commercial software HFSS was employed. For simplicity, the applied DC magnetic field was assumed to be uniform in all studied cases. The measurement process with some experimental restrictions was done for different DC magnetic bias values.

Throughout the whole study, we spotted the tunability and nonreciprocity of the reported ferrite CRLH couplers. The introduced results show that the different coupler types illustrate different new coupling propagation mechanisms with different propagation levels. Novel CRLH backward CLC performance has been explored. Also, a novel compact and nonreciprocal forward CLC is introduced here for the first time. As novel applications of the reported couplers types, it has been explained that such couplers can function as a novel microwave power switch with different possible designed power switching mechanisms[81]. Furthermore, the proposed horizontally magnetized CPW couplers require lower DC magnetic bias

compared to ferrite microstrip configurations.

II- LH Symmetrical Coupled Line Coupler Theory

The performance of the symmetrical CRLH CLC can be explained using the coupled mode approach[80]. The coupled mode equations for the forward and backward modes along the two identical CRLH coupled lines can be given as:

$$\frac{\partial a_1^+}{\partial z} = -j\beta_{LH}\, a_1^+ + jC_{BW}\, a_2^- - jC_{FW}\, a_2^+ \quad (1)$$

$$\frac{\partial a_2^-}{\partial z} = +j\beta_{LH}\, a_2^- - jC_{BW}\, a_1^+ + jC_{FW}\, a_1^- \quad (2)$$

$$\frac{\partial a_1^-}{\partial z} = +j\beta_{LH}\, a_1^- - jC_{BW}\, a_2^+ + jC_{FW}\, a_2^- \quad (3)$$

$$\frac{\partial a_2^+}{\partial z} = -j\beta_{LH}\, a_2^+ + jC_{BW}\, a_1^- - jC_{FW}\, a_1^+ \quad (4)$$

Where a_n^+ and a_n^-, with subscript n = 1,2 referring to the parallel lines 1 and 2 respectively, are the forward propagation and backward coupled mode waves, βLH the propagation constant of the individual CRLH lines, CBW the backward coupling coefficient, and CFW the forward coupling coefficient defined as:

$$C_{BW} = \beta_{RH}\left(\frac{\kappa_e + \kappa_m}{2}\right) \quad (5)$$

$$C_{FW} = \beta_{RH}\left(\frac{\kappa_e - \kappa_m}{2}\right) \quad (6)$$

$$\kappa_m = \frac{L_m}{L_R} \quad (7)$$

$$\kappa_e = \frac{C_e}{C_R} \quad (8)$$

According to the value and sign of the previous magnetic coupling coefficient, the mechanism of the CRLH CLC is established. Consequently, the CLCs are classified into either:

1- A typical backward coupler that has positive κm equal to κe, requiring a positive mutual inductance described as:

$$\kappa_m = \kappa_e \Rightarrow L_m = \frac{L_R}{C_R} C_e \quad (9)$$

Also, the backward coupling coefficient is described as:

$$C_{BW} = \frac{L_m}{L_R}\beta_{RH} \quad (10)$$

In general, the size of a coupled line coupler depends on the operation frequency. The lower the frequency, the larger the size. This is because the length of the two coupled lines of the coupler must have an electrical length of 90°, i.e., λ/4 physical lengths. If the two coupled lines are made of left-handed transmission lines, the physical length of the lines can be much smaller than λ/4, hence much smaller coupler can be realized[9]. As will be spotted later, the analysis of the backward CRLH coupled line coupler has revealed that the backward coupling lies within the stopband coupled mode propagation constants[80]. Consequently, the backward coupling will not be related to the electrical length, but to the attenuation length of the coupled lines. Therefore, CRLH backward CLC can achieve arbitrary coupling levels up to 0 dB.

2- A typical forward coupler that has negative κm equal to -κe requiring a negative mutual inductance described as:

$$\kappa_m = -\kappa_e \Rightarrow L_m = -\frac{L_R}{C_R} C_e \quad (11)$$

It has been understood that CRLH forward CLC can introduce higher electrical lengths at lower frequencies[73].

3- A general coupler with no constraints on either κm or κe.

III- Ferrite CRLH Coupled Line Coupler Concepts

Ferrite substrate has a dispersive relative permeability which can be either positive or negative quantity according to the ferrite magnetization and the applied DC magnetic bias. The negative permeability of a ferrite planar TL can represent a negative series parasitic inductive load, numerically, within its frequency bandwidth[49]. Therefore, the magnetic coupling coefficient, κm, between two planar parallel coupled TLs will change in sign and magnitude within this frequency bandwidth. As a result, the coupling mechanism of a planar CRLH CLC designed on a ferrite substrate will be frequency dependent according to the applied DC magnetic bias. In other words, it will vary according to the hosting ferrite TL permeability value.

Within the frequency band characterized by a positive permeability of the individual hosting ferrite TL (μ_f), the parasitic inductance of individual CRLH TLs is positive, like conventional TLs, and hence the coupler can demonstrate a positive magnetic coupling coefficient (κm). Then the CLC can be designed as a typical backward coupler by the proper design of the individual TL elements, the mutual inductance, and capacitance. But, within the frequency band characterized by a negative permeability of the individual hosting ferrite TL (μ_f), the parasitic inductance of individual CRLH TLs becomes negative, and hence the coupler can demonstrate a negative magnetic

coupling coefficient, κm. As a result, the coupler can no longer demonstrate a backward coupling mechanism within the negative ferrite permeability frequency band. Instead, the coupler is suitable to be designed as a typical forward CLC. On the other hand, the through propagation of a ferrite CLC is possible without any frequency band restriction, depending on the design requirements. Moreover, it has nonreciprocity propagation characteristics within the negative permeability frequency band of the hosting ferrite individual TLs depending on the propagation direction and the applied DC magnetic bias direction.

These previous notes can lead to introducing new properties of novel couplers having novel coupling and propagation properties. First, the cut-off frequencies of the negative ferrite permeability bandwidth can be used to determine the operational cut-off frequencies of a compact CRLH backward CLC. Second, a compact CRLH forward CLC can be designed within the negative permeability bandwidth of the individual hosting coupled TLs which can not be obtained using either an RH ferrite coupler or a CRLH dielectric coupler. Also, the concept of no backward coupling power within the negative permeability bandwidth can be utilized to switch power from the backward output port to either the through or forward coupling ports, according to the design objective. Hence, a novel power switch can be designed, which has not been proposed before. Finally, by controlling the DC magnetic bias direction and value, these proposed ferrite CLCs can also demonstrate tunable and nonreciprocity characteristics. All the proposed CLCs in this paper were implemented using CPW configuration over ferrite substrate. The vertical cross-section for all cases is shown in Fig. 1. The used ferrite substrate in the design is Trans Tech G-113* with substrate thickness (h) = 1 mm. The electrical and magnetic parameters of this ferrite substrate material were introduced in chapter 4.

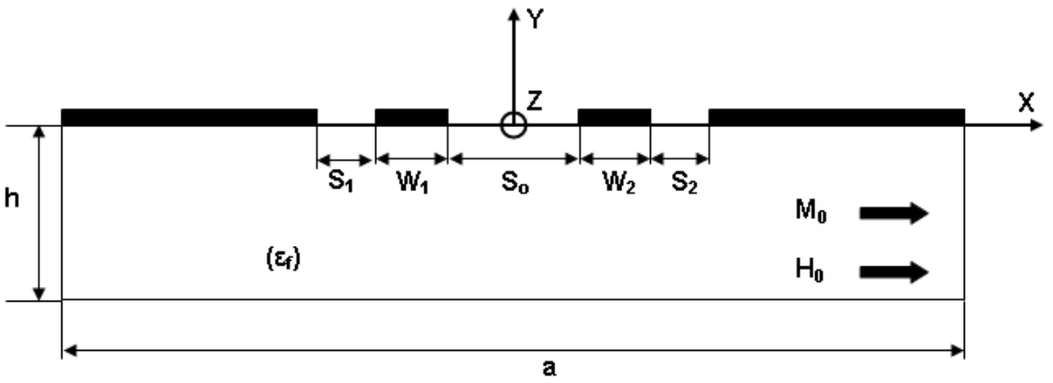

Fig. 1: The vertical cross-section of all CRLH CPW CLCs.

For all types, an internal DC magnetic field (H_0) is applied to the ferrite substrate in the shown direction in Fig. 1 causing the ferrite substrate to have saturation magnetization in the same direction. For the shown direction of DC magnetic bias, the equivalent relative ferrite permeability of the ferrite hosting CPW TL (μ_f) is equal to (μ_{fn}) defined in (12). This equivalent permeability is negative within the frequency range $f_{nl} < f < f_{nh}$ where f_{nl} and f_{nh} were calculated using equations (13) and (14), respectively.

$$\mu_{fn} = \mu \tag{12}$$

$$f_{nl} = \frac{1}{2\pi}\omega_h \tag{13}$$

$$f_{nh} = \frac{1}{2\pi}\omega_{hm} \tag{14}$$

IV- Nonreciprocal Dual Mode Backward CLC

In this section, we present a novel dual-mode and nonreciprocal ferrite CRLH backward CPW CLC[66,68,81]. The proposed coupler was designed using two identical CRLH TLs formed using shunt planar strip inductors and series interdigital capacitors over a ferrite substrate. The coupler's through output and the backward coupling output are located in two separated bands. The first mode was designed to demonstrate a reciprocal backward coupling propagation with almost 0 dB coupling level in the first band. On the other hand, the second band has nonreciprocal through propagation. Moreover, the proposed coupler performance can be tuned by changing the applied DC magnetic bias. Hence a novel power switching between the backward output port to the through output one can be achieved. This novel microwave application can be obtained by only changing the DC magnetic bias of the dual-mode coupler.

Such a coupler with this high backward coupling level

cannot be achieved using conventional ferrite CLC. Also, nonreciprocal through propagation cannot be achieved using dielectric CRLH CLC. Therefore, the proposed coupler can be considered a unique coupler which cannot be achieved using another coupler configuration. Through our study of the CLC in this section, we start by summarizing the generalized coupled mode approach explanation for novel coupling properties of a CRLH backward CLC[80]. Then, we modify this approach to be applied in case of a ferrite CRLH backward CLC. Next, the performance of the proposed coupler was explained theoretically, verified numerically, and confirmed experimentally.

A- LH backward CLC concepts

The CRLH backward CLC performance can be explained using the generalized coupled mode approach assuming the forward coupling coefficient CFW = 0[80]. Therefore, the coupled mode equations for backward modes along the two coupled lines can be simplified from equations (1) to (4) as:

$$f_{nh} = \frac{1}{2\pi}\omega_{hm} \tag{15}$$

$$\frac{\partial a_2^-}{\partial z} = +j\,\beta_{LH}\,a_2^- - j\,C_{BW}\,a_1^+ \tag{16}$$

Through the coupled mode approach analysis, the propagation constant along the coupled lines has been derived, found to be identical to those of the even/odd mode circuits as[80]

$$\beta_{I,II} = \sqrt{\beta_{LH}{}^2 - C_{BW}^2} \tag{17}$$

The CRLH backward coupler scattering matrix parameters have been proven in[80] as:

$$S_{11} = 0 \tag{18}$$

$$S_{21} = \frac{A e^{-j\beta_I l} + B e^{-j\beta_{II} l}}{A + B} \tag{19}$$

$$S_{31} = \frac{A(\beta_I - \beta_{LH})\, e^{-j\beta_I l} + B\,(\beta_{II} - \beta_{LH})\, e^{-j\beta_{II} l}}{A(\beta_I - \beta_{LH}) + B(\beta_{II} - \beta_{LH})} \tag{20}$$

$$S_{41} = 0 \tag{21}$$

Where A and B are constants. From (17), it has been explained that the coupled lines propagation constant may be imaginary at some frequencies[80]. Hence, from (20), it can be seen that a 0 dB backward coupling is possible within these frequency bands.

B- Ferrite CRLH backward CLC theory

In our ferrite CRLH backward CLC works; the ferrite was used as a substrate, and the left-handed propagation constant is defined in terms of the ferrite medium as in (22).

$$\cos(\beta_{LH}\, d) = 1 - \frac{1}{2}\omega^2 d^2 \left(\mu_o\,\mu_f - \frac{1}{\omega^2 C_L\, d}\right)\left(\varepsilon_o\,\varepsilon_f - \frac{1}{\omega^2 L_L\, d}\right) \tag{22}$$

The mutual inductance, Lm, and the backward coupling coefficient, CBW, can be defined in terms of the medium parameters using (9) and (10), respectively, as follows;

$$L_m = \frac{\mu_0\,\mu_f}{\varepsilon_0\,\varepsilon_f} C_e \tag{23}$$

$$C_{BW} = \omega \sqrt{\frac{\varepsilon_o\,\varepsilon_f}{\mu_o\,\mu_f}}\, L_m \tag{24}$$

From (22) and (23), it is clear that both the backward coupling coefficient, CBW, and the propagation constant of individual CRLH transmission lines, βLH, are dispersive quantities due to the dispersive ferrite permeability. Thus, using (17), the propagation constants of the propagating waves along the coupler have a dispersive nature. Due to these dispersive properties, in addition to the nonreciprocal properties of hosting ferrite TL within its negative permeability frequency band, a CRLH backward CLC implemented on ferrite substrate is expected to have a tunable and nonreciprocal performance by varying the applied DC magnetic bias.

C- Nonreciprocal dual mode backward CLC theory

As explained before, a CRLH CLC is capable of demonstrating a 0 dB backward coupling level. Also, it has been understood that a ferrite CRLH backward CLC can not support backward coupling within the frequency band of negative permeability of individual hosting ferrite TLs[66,81]. Therefore, from these two conclusions, a ferrite CRLH backward CLC can be designed such that it demonstrates an almost 0 dB coupling level within a certain frequency band characterized by positive ferrite permeability. For a particular DC magnetic bias value, the onset of the negative ferrite permeability can be used to determine the cut-off of the desired backward coupler. For frequencies higher than this cut-off frequency, the propagation mechanism can be designed to have only through propagation. Also, the through propagation direction of the coupler can be selected to be in the direction of the non-evanescent nonreciprocal through propagation within the frequency band of negative ferrite permeability.

Accordingly, the principle of operation of our current coupler is to utilize the onset of the negative permeability to set up the upper cut-off frequency of backward coupling propagation demonstrating almost 0 dB backward coupling level, i.e., first mode. Also, this frequency can be designed

as the lower cut-off frequency of the nonreciprocal through propagation, i.e., the second mode. This is to say in optimum design; theses two cut-off frequencies should overlap with each other.

Moreover, since the negative permeability onset frequency of the individual hosting ferrite TLs determines the cut-off frequencies of the different modes, thus the coupler can be tunable by varying the DC magnetic bias. As a new application, a novel microwave output power switch from the backward output port to the through one within a specific frequency band can be achieved by using two suitable DC magnetic bias values.

D- Nonreciprocal dual mode backward CLC structure

The detailed layout diagram of the proposed nonreciprocal dual mode CRLH CPW CLC is shown in Fig. 2 (a). The coupler was designed using two identical CRLH TLs separated by a distance S_0. Each CRLH TL was designed using a simple shunt straight strip inductor and series interdigital capacitor whose detailed dimensions are illustrated in Fig. 2 (b). The series load interdigital capacitor has six fingers. Two identical interdigital capacitors are used at both the input and the output of the coupler whereas the one between the two periodic cells has double length, ta, and double air gap between the capacitor fingers and the periodic cell end, tac, compared to the dimensions of the two capacitors at both ends. Otherwise, all interdigital capacitors have the same finger width, W_c, and separation, S_c. These different capacitor configurations were used for matching purposes. Extension legs of the two coupled lines are added at each line at each port for the proper simulation of the real case of the fabricated circuit. The dimensions of all CPW TL extension legs are identical such that they represent a 50 Ω TL. Finally, an internal horizontal DC magnetic field (H_0) is applied to the ferrite substrate.

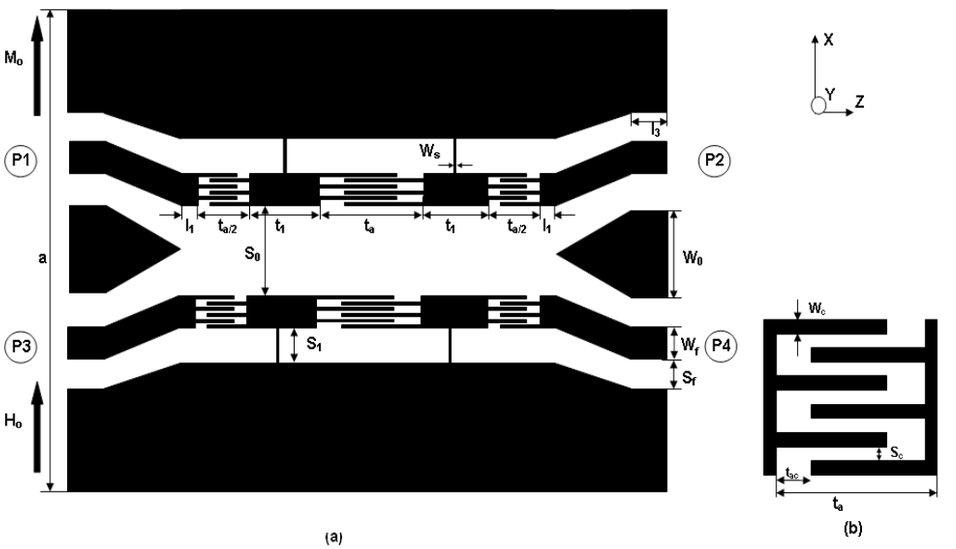

Fig. 2: (a) The layout geometry of the ferrite CRLH CPW CLC, a=19.8mm, L=10.2 mm, W_0= 6mm, t_a =2.mm, t_1 =1.5mm, l_1 =0.25mm, S_0=0.5mm, S_f=0.8mm, W_f=1.3mm, W_s= 0.25 mm, and l_3=0.1 mm (b) The interdigital capacitor geometry S_c=W_c=0.1mm and t_{ac}=0.2 mm[66].

E- Nonreciprocal dual mode backward CLC design

The design procedures of the proposed dual-mode ferrite CRLH CPW CLC can be fulfilled in three main steps. The first step is designing a wide band almost 0 dB backward CLC. This step can be achieved using the general principles of arbitrary coupling level of conventional CRLH backward CLCs. The circuit design of the coupler was fulfilled using comprehensive circuit optimization of its equivalent circuit whose half-symmetric section is shown in Fig. 3. Accordingly, the lumped elements of both of loading elements and the parasitic ones were designed such that the even and odd modes are not propagating within the desired coupling bandwidth.

In the second step, the ferrite CPW CLC structure was designed physically utilizing real loading elements. The loading elements, whose values were obtained from the above circuit simulation, were obtained analytically as a start. The interdigital capacitors were calculated using[9], the inductors using[78], and the CPW parasitic elements using[67]. Such structure was optimized using HFSS assuming a very high DC magnetic bias applied to the hosting ferrite substrate.

Then, by further circuit optimization of the proposed coupler equivalent circuit and comparing its response to the optimized HFSS numerical results, an initially designed isotropic CRLH CPW CLC can be obtained. At this stage, the exact loading and parasitic elements were obtained by curve fitting the aforementioned two simulation results.

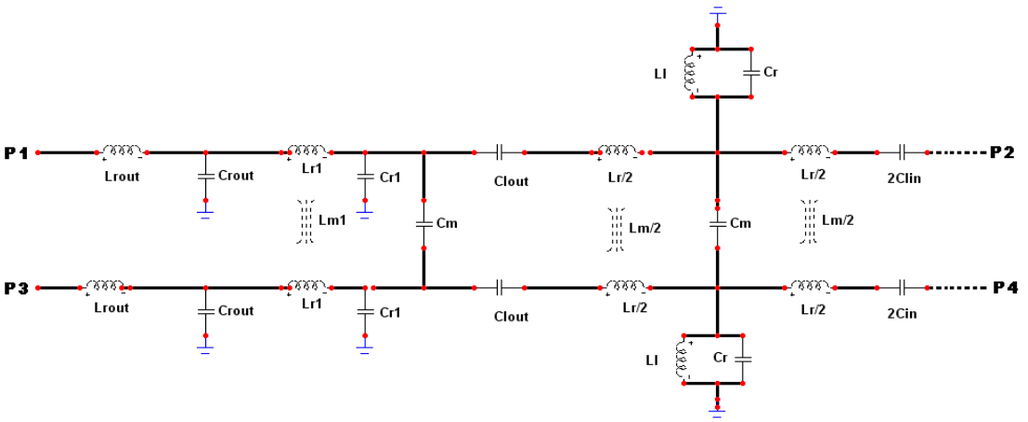

Fig. 3: The equivalent circuit of the dual mode ferrite CRLH CPW CLC.

The final step of the design of the dual mode nonreciprocal ferrite CRLH CPW CLC was obtained through further optimization of the initially designed isotropic CLC assuming lower DC magnetic bias values applied to the ferrite substrate. The basic concept of this optimization is to make use of, first, the property of 0 dB CRLH backward coupling to introduce the first operating band demonstrating almost 0 dB backward coupling level and, second, from the nonreciprocal propagation properties of the hosting ferrite CPW TL to introduce the second operating band having nonreciprocal through propagation. Therefore, the applied DC magnetic bias direction was selected such that the through propagation direction, assuming excitation at port (1), is the non-evanescent propagation direction within the negative ferrite permeability frequency band. For optimum design, the upper cut-off frequency of the 0 dB backward coupling propagation and the lower one of the through propagation coincide with the negative permeability onset frequency of the hosting ferrite CPW TL. Since this cut-off frequency is dependent on the applied DC magnetic bias, hence the bias value can control the switching mechanism between the 0 dB backward propagation and the nonreciprocal through propagation within a specific bandwidth. Accordingly, a novel microwave power switch can be achieved.

F- Nonreciprocal dual mode backward CLC numerical results

The simulated scattering parameters of the initial design of the proposed coupler using HFSS for H0=50,000 Oe, which represents a very high DC magnetic bias value as explained earlier in the design procedures, are shown in Fig. 4. Simultaneously, its optimized equivalent circuit simulation results are illustrated in the same figure for comparison purposes. The initial coupler structure has the same dimensions as those in Fig. 2 except t_l=1.1 mm, t_a=1.8 mm, and L=9 mm. The figure shows a reasonably good agreement between the two simulated results, especially for the backward coupling level. The backward coupling level is approximately -1 dB, within the frequency band from 5 GHz to 9 GHz. Considering the HFSS results, we can conclude within that frequency bandwidth, the coupler has approximately better than -10 dB reflection coefficient, through propagation level below -12 dB, and better than 20 dB forward coupling isolation difference.

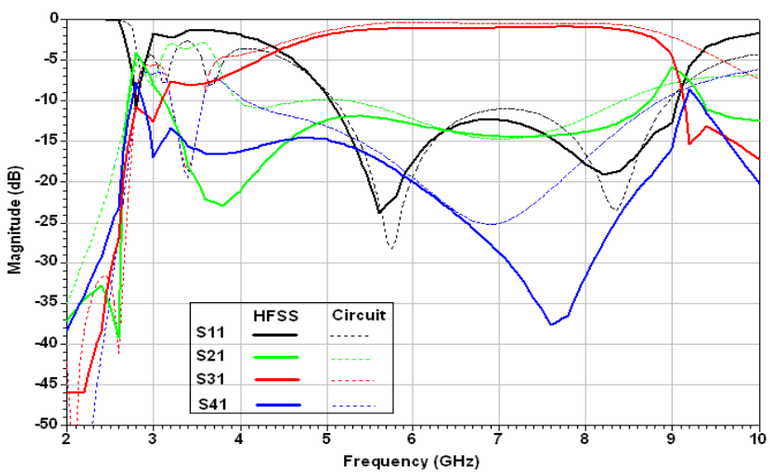

Fig. 4: HFSS and equivalent circuit modeling simulated scattering parameter magnitudes of the initial proposed dual-mode CPW CLC, HFSS for H_0=50,000 Oe (solid line) and circuit model (dotted line), C_{Lout}=1.6 pF, C_{Lin}=1.2 p_F, L_L=0.45nH, K_m=0.5, C_c=1.4 pF, C_r=0.4 pF, C_{rl}=0.1 pF, C_{rout}=0.4 pF, L_r=0.7 nH, L_{rl}=0.4 nH, and L_{rout}=0.25 nH.

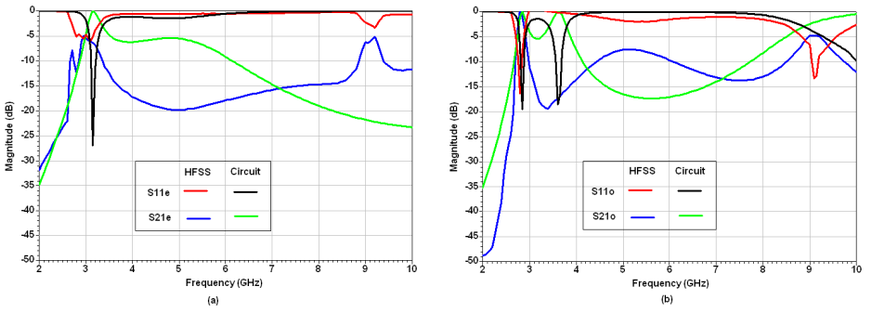

Fig. 5: HFSS simulation and circuit modeling simulation for the scattering parameter magnitudes of the dual mode ferrite CRLH CPW CLC, HFSS for H_0=50,000 Oe (solid line) and circuit model (dotted line) (a) Even lines (b) Odd lines.

The design of the coupler was assured by achieving non-propagation for both the even and odd modes along the coupler. The simulated even and odd mode magnitudes using both HFSS and circuit simulations are shown in Fig. 5 (a) and (b), respectively. It can be confirmed that both simulations demonstrate almost 0 dB even and odd mode return loss within the frequency bandwidth from 3.5 GHz to 8 GHz which is overlapped with the full backward coupling propagation bandwidth shown in Fig. 4. This frequency band extends to more than 9 GHz for the odd mode. However, there is a significant difference between the two simulated transmission coefficient levels (S21) for both even/odd modes. Such levels can reflect a very small transmission power as both are less than -10 dB over most of the coupled bandwidth. In other words, these differences do not affect the desired almost 0 dB return loss. These results confirm the validity of that equivalent circuit representing the proposed 0 dB CRLH CLC within this frequency bandwidth.

The second step explained in the design procedures is to optimize the coupler structure for the proper design objectives under lower DC magnetic bias values. The optimization study has been done for different geometry parameters of loading elements and parasitic elements to achieve approximately 0 dB backward coupling with high nonreciprocity and forward coupling isolations for the two propagating modes around H_0=2000 Oe. The HFSS simulated scattering parameters of the optimized dual mode coupler for H_0= 2000 Oe are shown in Fig. 6. The results show a backward propagation with a very close to 0 dB level over a frequency bandwidth that extends from 3.4 GHz to 6 GHz. Then it decreases from approximately -3 dB at 6 GHz with a very high slope to reach approximately -15 dB at 6.5 GHz. Following the backward propagation passband, the coupler has through propagation, no stopband separates them. On contract to the backward coupling performance, the through level increases from approximately -13 dB at 6 GHz up to -5 dB at 6.5 GHz with nonreciprocal propagation with a nonreciprocity isolation level that extends up to 30 dB at 7.5 GHz. However, the through propagation level is some how lossy compared to the backward coupling in the first band due to the lossy nature of the ferrite substrate within the negative permeability frequency band. Finally, the coupler has a low forward coupling signal (S41) whose isolation level is better than 20 dB over most of the operating bandwidths. It can be observed that the cut-off of the backward coupling propagation is the onset frequency of the nonreciprocal through propagation, where the negative ferrite permeability frequency band appears. This frequency for H_0=2000 Oe can be calculated approximately using (12) to be 5.6 GHz.

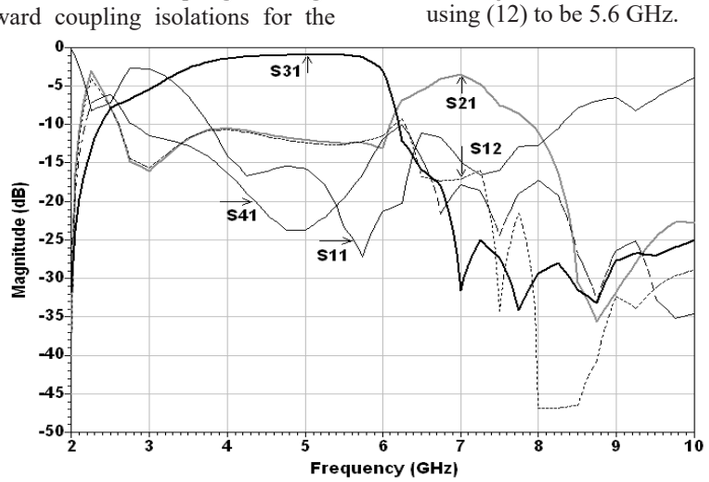

Fig. 6: The full wave simulated scattering parameter magnitudes of the dual mode ferrite CRLH CPW CLC for H_0=2000 Oe.

As the upper cut-off frequency of the backward coupling propagation coincides with the onset of the negative permeability of the hosting CPW ferrite TL, the coupler can be tunable by changing H_0. The scattering parameters of the coupler were simulated again for different values of H0 as shown in Fig. 7. The figure illustrates that the coupler demonstrates tunable dual-band and nonreciprocal propagation performance similar to the previous optimized case. The closer H_0 to 2000 Oe cases have similar optimum performance. For the H_0=1500 Oe case shown in Fig. 7 (a), the 3 dB upper cut-off frequency of the backward coupling is shifted down to approximately 5 GHz. The start of the through propagation, with a little below -10 dB level, is at 5.5 GHz and it continues with nonreciprocal propagation to approximately 6.5 GHz. For H_0=1750 Oe, as illustrated in Fig. 7 (b), the 3 dB upper cut-off frequency of the backward coupling is increased to approximately 6 GHz. The start of the through propagation, with a -10 dB level, is at 6 GHz and it continues with nonreciprocal propagation to approximately 7 GHz. As illustrated in Fig. 7 (c) for H_0=2250 Oe, the 3 dB upper cut-off frequency of the backward coupler propagation is increased to approximately 6.5 GHz. A nonreciprocal through propagation exists within the frequency band from 6 GHz to approximately 8 GHz. Finally, for H_0=2500 Oe, the simulated scattering parameters of the coupler are shown in Fig. 7 (d). The 3 dB cut-off frequency of the backward coupling is at 6.5 GHz whereas the through one with approximately -10 dB level starts at 7 GHz. It is observed that the nonreciprocal characteristics of the through propagation are non-significant at the start of its propagation bandwidth, from 7 GHz to 7.7 GHz. Then it becomes more significant with more than 20 dB nonreciprocity isolation found.

Finally, we can claim that a reciprocal backward coupling requires a positive relative permeability of the hosting ferrite CPW TL. In other words, backward coupling propagation is not possible in the frequency bandwidth of its negative ferrite permeability. On the other hand, a nonreciprocal through propagation requires a negative one. To confirm these conclusions, the same coupler was studied assuming a very high DC magnetic bias applied to the ferrite substrate, H_0=50,000 Oe; the hosting CPW TL has always positive unity relative permeability. The simulated scattering parameters of the proposed coupler, in this case, are shown in Fig. 8 where it is obvious that the coupler has only one operating frequency band that extends up to 7.5 GHz and it has only backward coupling propagation within that band. Following this band is perfect stopband propagation with return loss close to 0 dB.

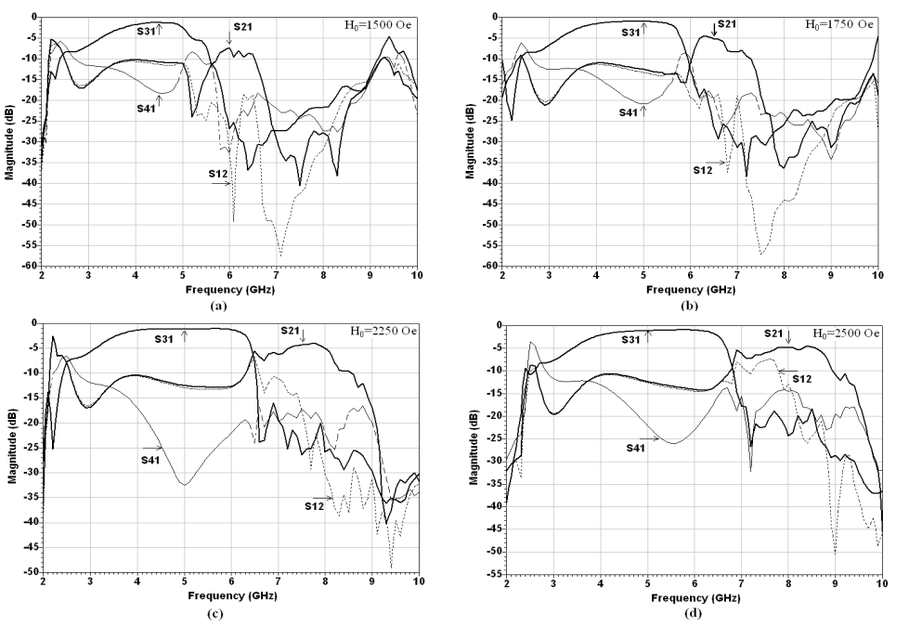

Fig. 7: The full wave simulated scattering parameter magnitudes of the dual mode ferrite CRLH CPW CLC for (a) H_0=1500 Oe, (b) 1750 Oe, (c) 2250 Oe, and (d) 2500 Oe.

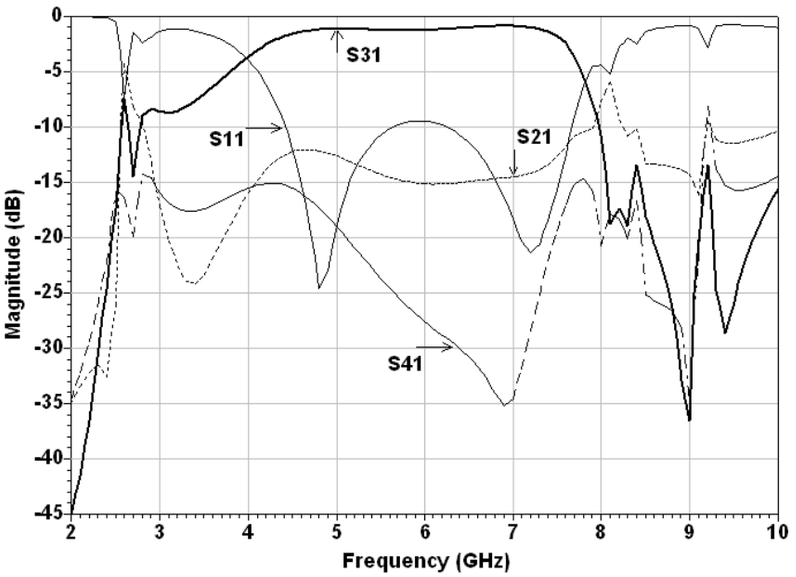

Fig. 8: The full wave simulated scattering parameter magnitudes of the dual mode ferrite CRLH CPW CLC for H_0=50,000 Oe.

G- Nonreciprocal dual mode backward CLC measurement results

For confirming the predicted performance of the proposed dual-mode ferrite CRLH CLC coupler, the coupler has been realized and measured. The measurement experimental setup is set since the coupler is a 4-port circuit, it was measured as a 2-port network while the other two ports were matched to a 50 Ω load. This process was repeated for each couple of ports to be measured (6 different combinations).

The fabricated coupler was realized using the commercial YIG Trans Tech TTVG-1850 as the substrate material. The utilized ferrite substrate was defined in terms of its electric and magnetic properties the same as in chapter 6, expressing high similarity with the originally designed one G-113*. The dimension of this bulk material is 19 mm x 13 mm x 1 mm. The feeding CPW TL length l3 is increased to 1.5 mm instead of 0.1 mm for the sake of SMA connection limitation.

Two horizontal FR4 PCB boards with 1.5 mm thickness, used as circuit covers, were soldered to the SMAs. The lower cover is 0.6 mm beneath the substrate bottom while the upper cover is 1.9 mm above the printed circuit layout. This fabricated circuit prototype is shown in Fig. 9 (a). The soldered circuit prototype employing a lower FR4 cover is shown in Fig. 9 (b) whereas, the two-sided circuit prototype is shown in Fig. 9 (c). Also, the horizontal circuit orientation between the two electromagnet poles with the four connection cables is shown in Fig. 10.

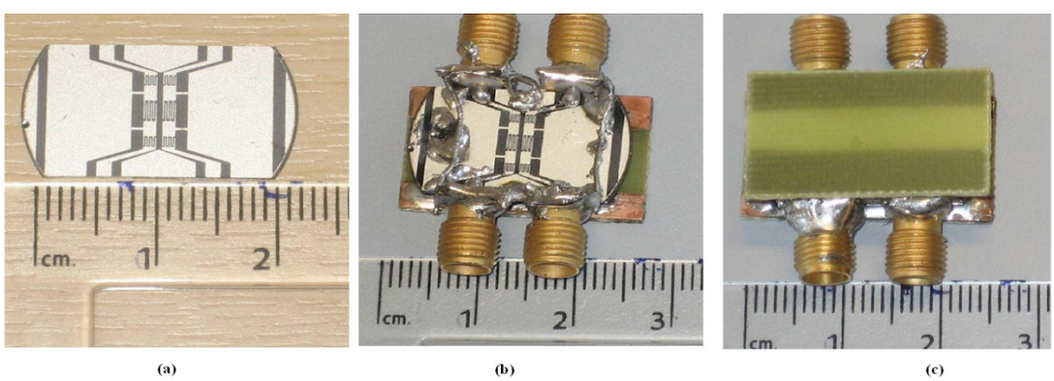

Fig. 9: The TTVG-1850 dual mode ferrite CRLH CPW CLC (a) The circuit prototype (b) The lower-sided covered circuit prototype (c) The two-sided covered circuit prototype

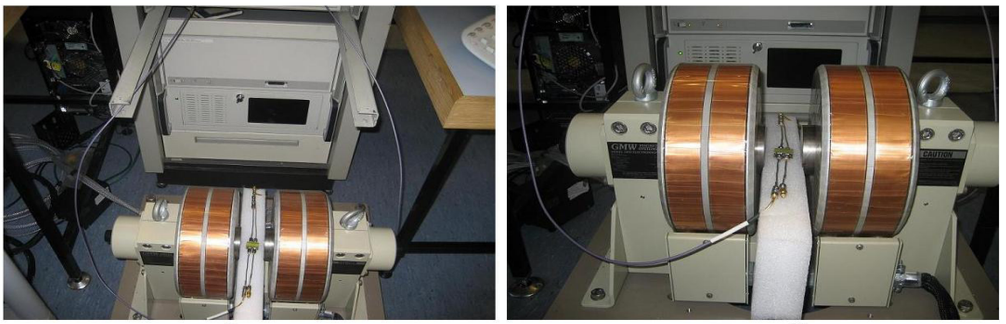

Fig. 10: The dual mode ferrite CRLH CPW CLC circuit measurement setup (a) Vertical view (b) Front view.

To compensate for the demagnetization field, the external field was increased by 90 Oe in all studied cases [82]. The measurement results for the proposed coupler for H_0 = 2000 Oe are shown in Fig. 11. In general, the propagation suffers from a high reflection at frequencies up to 6 GHz, S11 level is an average of -3 dB. Beyond this frequency, S11 decreases to be approximately less than -10 dB with some decreasing peaks of -18 dB and -15 dB at 6.6 GHz and 7 GHz, approximately. Apart from that high reflection level, the figure illustrates that the proposed coupler has two different propagation passbands. A reciprocal backward coupling propagation is allocated within the first passband whereas a nonreciprocal through propagation is within the second passband. In other words, despite the introduced high reflection, the coupler functionality is still obvious. This high reflection level affects the designed two modes' passband levels. Such an effect is very significant in the first reciprocal backward coupling passband. The poor matching at measurements can be explained due to the effect of the measured configuration which was very urgent for avoiding circuit damage while measurements.

The reciprocal backward coupling propagation starts from 3 GHz, approximately. Its level reaches its maximum of -5 dB at 3.5 GHz then it decays to -10 dB at 3.9 GHz and further decreases to -15 dB at 4.5 GHz. The reciprocal backward coupling propagation suffers from a resonance whose peak value is at 5.2 GHz, and its level increases again to more than -10 dB within the frequency band 5.8 GHz to approximately 6.5 GHz. An explanation for that behavior is that the measured device configuration causes some parasitic resonance for the backward coupling propagation around 5 GHz. This explanation will be verified later. Higher than 6.5 GHz, the backward coupling dramatically decreases to very lower values at higher frequencies.

On the other hand, the through propagation within that frequency band is below -20 dB. The second passband is apparent from approximately 6 GHz above which the backward coupling propagation starts to decay and the coupler demonstrates only through propagation. Such propagation becomes completely nonreciprocal at 6.5 GHz up to 8 GHz with almost -10 dB through propagation level (S21). The average nonreciprocity isolation difference in this band is better than 10 dB; it is low at the bandwidth beginning and increases with the frequency increase.

It is evident, however, these measurement results show significant variations by comparing them with their HFSS simulated ones, shown in Fig. 6. These variations can be explained due to the difference between the typically designed simulated and practical measured structures. For confirming such structure differences effect, the measured structure was numerically simulated using HFSS for H_0=2000 Oe and its scattering parameters magnitudes are shown in Fig. 12. In general, the simulated structure shows the dual mode propagation phenomenon of the proposed coupler. However, the reflection coefficient is very high compared to the ideal design, shown in Fig. 6, especially from 4.8 GHz. It is noted that a high reflection was also observed in the measurement results in Fig. 11, although they are not identical. This can confirm the imperfect matching condition of the housing measured structure.

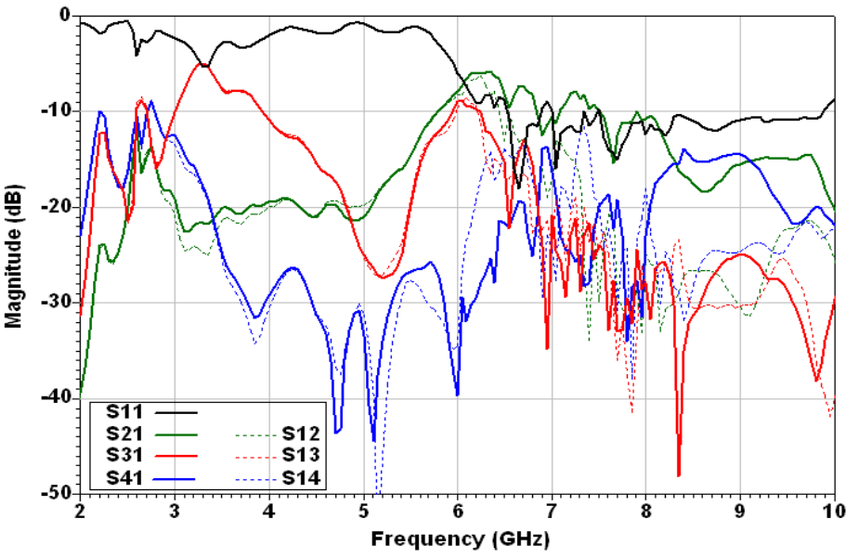

Fig. 11: The measured scattering parameter magnitudes of the dual mode CRLH CPW CLC for H_0= 2000 Oe.

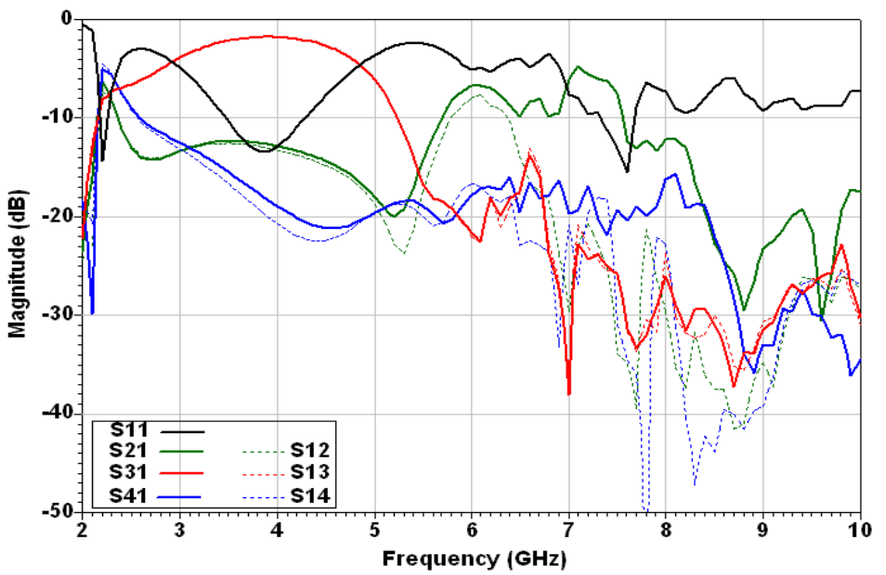

Fig. 12: The full wave simulated scattering parameter magnitudes of the measured structures dual mode ferrite CRLH CPW CLC for H_0=2000 Oe.

For more emphasis on the proposed coupler performance and its predicted tunable performance, introduced in both theoretical and numerical analysis, it has been measured for different H0 values around H0 =2000 Oe. The measurement results for the proposed coupler for H_0 = 1500 Oe, 1750 Oe, 2250 Oe, and 2500 Oe are shown in Fig. 13.

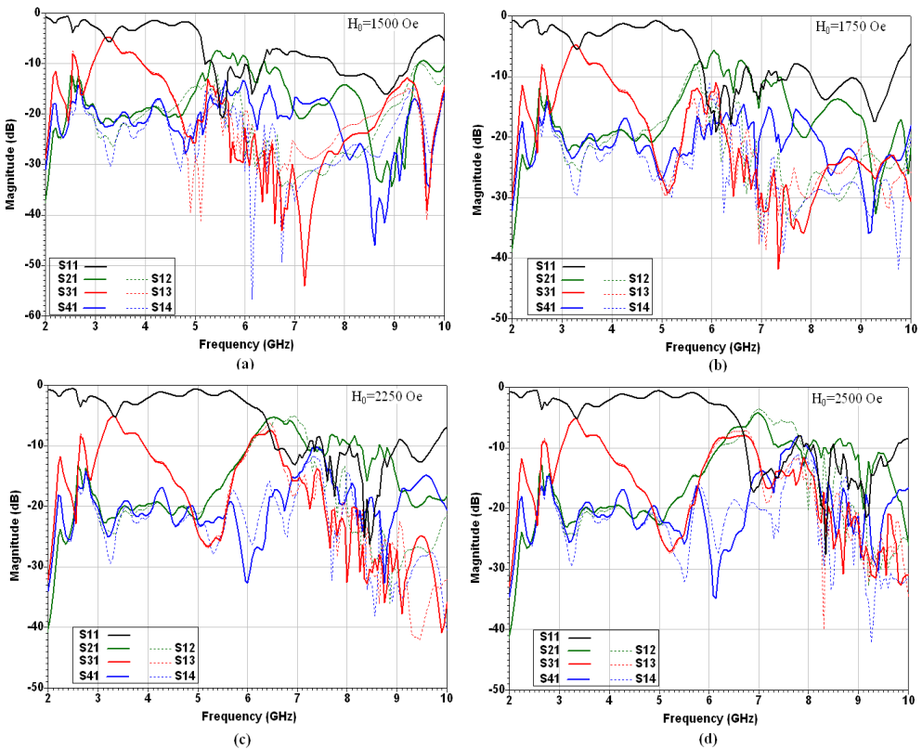

Fig. 13: The measured scattering parameter magnitudes of the dual mode CRLH CPW CLC for (a) 1500 Oe, (b) 1750 Oe, (c) 2250 Oe, and (d) 2500 Oe.

For H_0=1500 Oe, as shown in Fig. 13 (a), the reciprocal backward coupling propagation starts from 3 GHz, approximately. Its coupling level reaches its maximum of -5 dB at 3.3 GHz. Then it decays to -10 dB at 3.95 GHz and further decreases to -22 dB at 5 GHz. Then, the level increases again to -15 dB in a very narrow bandwidth, from 5.2 GHz to 5.3 GHz before it decreases very rabidly at higher frequencies. On the other hand, the through propagation within that frequency band is below -20 dB before it starts to increase to become higher than -10 dB at 5.4 GHz. It can be seen that only a nonreciprocal through propagation exists in the second band up to 6.5 GHz. Also, the average nonreciprocity isolation difference in this band is better than 10 dB. However, the forward coupling isolation difference in that second passband is a little bit less than 10 dB.

Next, the measurement results for H_0=1750 Oe are shown in Fig. 13 (b). The reciprocal backward coupling propagation suffers from the parasitic resonance whose peak value is at approximately 5.1 GHz while it re-increases to approximately -13 dB over a wider frequency band compared to the previous case, 5.5 GHz to 6.3 GHz. The through propagation performance is similar to the above case. Its level is approximately -20 dB in the frequency band up to 5 GHz. Then it increases to be better than -10 dB at 5.6 GHz. It becomes nonreciprocal at 6 GHz and it extends approximately to 7.4 GHz with an average nonreciprocity isolation difference better than 10 dB.

For H_0=2250 Oe as shown in Fig. 13 (c), the resonance peak of the backward coupling propagation becomes wider and flat from 5 GHz to 5.4 GHz. The further backward coupling propagation increase becomes flatter with -8 dB in the frequency range of 6 GHz to 6.5 GHz. The through propagation distinguishing the second band starts at 6 GHz to 7.4 GHz with a level better than -10 dB and reciprocal nature. Then, it becomes nonreciprocal from 7.4 GHz to approximately 8.6 GHz.

Finally, the measurement results for H_0=2500 Oe are shown in Fig. 13 (d). Similar to the previous case, the resonance peak of the backward coupling propagation is still flat and wide from 5 GHz to 5.5 GHz. Also, the further backward coupling propagation increase is much wider and flat with -8 dB in the frequency range of 6 GHz to 6.8 GHz. The through propagation distinguishing the second band starts at 6 GHz to almost 8 GHz with a level better than -10 dB and reciprocal nature. Then, the complete nonreciprocal through propagation extends to approximately 9.5 GHz.

Can be observed significant variations by comparing these measurement results to their ideal designed ones using HFSS, shown earlier in Fig. 7. These variations have been explained above that it is due to the measured structure configuration effect, i.e. with PCB covers. For more confirmation of these structure configuration effects, the measured structure was numerically simulated using HFSS and the simulated results were compared to the measured ones for different DC magnetic bias values.

Accordingly, the comparisons, for both backward coupling and through propagations, are shown in Fig. 14, Fig. 15, and Fig. 16 for H_0=1500 Oe, 2000 Oe, and 2500 Oe, respectively.

In general, the simulated through propagation is approximately 7 dB higher than the measured one at low frequencies extending approximately up to 5 GHz at which little difference exists. This bandwidth should be within the first operating band of the dual-mode operation. Despite these variations, both results can be represented as no through propagation within this bandwidth. Beyond 5 GHz, both simulated and measured through propagation results are very close to each other. By comparing Fig. 14 (a) to Fig. 16 (a) for H_0=1500 Oe to 2500 Oe, respectively, we found that the lower the H_0 values the closer two compared curves. Also, all measured cases have slightly smaller nonreciprocity isolation levels compared to the simulated ones.

On the other hand, from Fig. 14 (b) to Fig. 16 (b), the simulated backward coupling propagation reaches approximately -4 dB at the center frequency in the first low-frequency bandwidth up to 5 GHz. Then, it decays rapidly at about 5 GHz due to the parasitic resonance before it increases again demonstrating another passband with narrower bandwidth and lower through propagation level compared to the ones in low-frequency bandwidth. Following, a stopband exists as a result of the dispersive negative permeability. By comparing these results to the measurement ones, we can observe that the measurement results can follow the same operation shape. However, the measured parasitic resonance decays more rapidly in the first low-frequency bandwidth. They are approximately no more than 7 dB lower than the simulated ones up to 4 GHz, but this difference increases by further frequency increase, it reaches more than 15 dB in the worst case. Also, the measured results have higher through propagation levels compared to simulated ones beyond the resonance peak frequency, the difference increases by increasing H_0 values. Excellent agreement between both measured and simulated results within the negative permeability stopband. As an example, for H_0=1500 Oe, both results are almost identical at frequencies higher than 5 GHz.

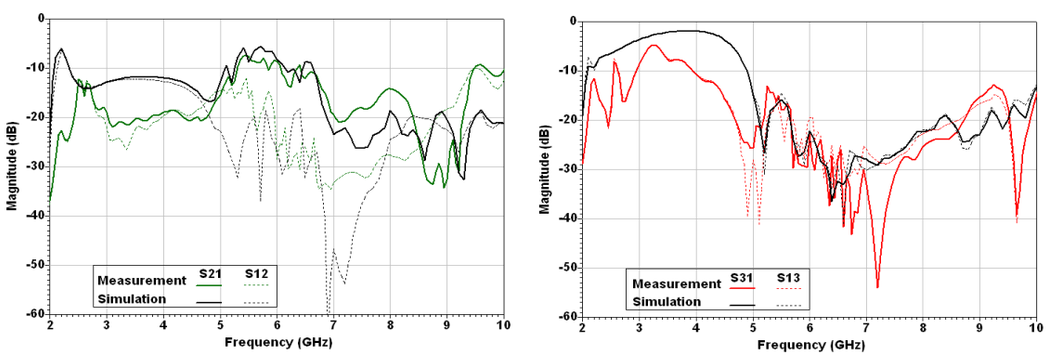

Fig. 14: The comparison between the dual-mode ferrite CRLH CPW CLC measurement results and the simulation ones for similar measured structure for H_0= 1500 Oe (a) Through comparison (b) Backward coupling comparison.

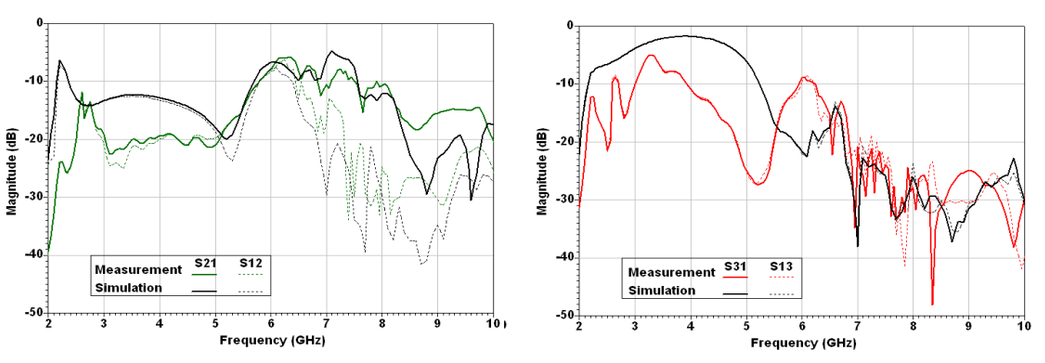

Fig. 15: The comparison between the dual-mode ferrite CRLH CPW CLC measurement results and the simulation ones for similar measured structure for H_0= 2000 Oe (a) Through comparison (b) Backward coupling comparison.

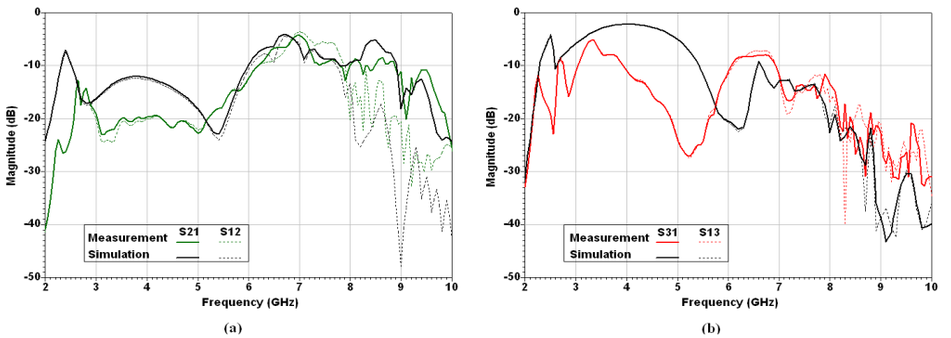

Fig. 16: The comparison between the dual-mode ferrite CRLH CPW CLC measurement results and the simulation ones for similar measured structure for H_0= 2500 Oe (a) Through comparison (b) Backward coupling comparison.

These comparison variations can be explained due to the effect of non-uniform DC magnetic bias; it was assumed uniform in HFSS simulations, whose effect becomes more significant with higher DC magnetic bias values[83]. Also, the structure of the housing of the circuits could have a quite effect. In the simulation, perfect radiation boundaries were assumed. In practice, however, the housing, such as the SMAs, and wires connected to the grounds are not what we simulated.

Finally, the switching mechanism of the proposed coupler controlled by the applied DC magnetic bias is introduced as another novel application of the proposed coupler. This switching mechanism can be made clear by examining the dual mode coupler response for H_0=0 as shown in Fig. 17. It can be observed that the backward coupling propagation is the dominant output signal with better than 10 dB through isolation difference, in the bandwidth 6.5 GHz to 7.5 GHz. By comparing this bandwidth to the cases of H_0=1750 Oe and 2000 Oe shown in Fig. 13 (b) and Fig. 11 respectively, we can observe that the dominant output power becomes the through one with more than 10 dB backward coupling isolation difference. Thus, we can conclude that this coupler can act as a novel microwave switch between the backward coupling and the through output ports in the frequency band 6.5 GHz to 7.5 GHz by simply changing H_0 from 0 Oe to 2000 Oe. This switching is made clearer in Fig. 18 which illustrates the switching between the backward coupling output (dotted green line) with H_0=0 Oe to the through output (solid red line) with H_0=2000 Oe within the frequency band 6.4 GHz to 7.4 GHz. Both two output levels are on average -9 dB.

Such a switching mechanism can be considered a novel microwave application. Better switching results and wider operating bandwidth can be expected through the circuit and full wave optimizations. In summary, a novel compact size dual mode nonreciprocal ferrite CRLH CPW CLC has been introduced. The proposed coupler demonstrates reciprocal backward coupling propagation mode at lower frequencies and nonreciprocal through propagation mode at higher frequencies. Theoretical analysis, numerical design results, and confirming measurement results of the proposed coupler were introduced. A completely novel microwave switch has been suggested as a new microwave application for this coupler.

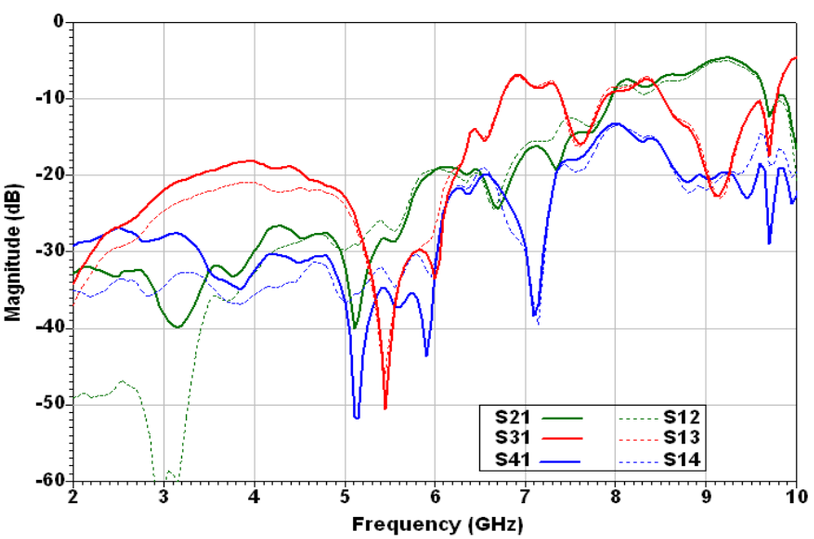

Fig. 17: The measured scattering parameter magnitudes of the dual mode CRLH CPW CLC for H_0=0

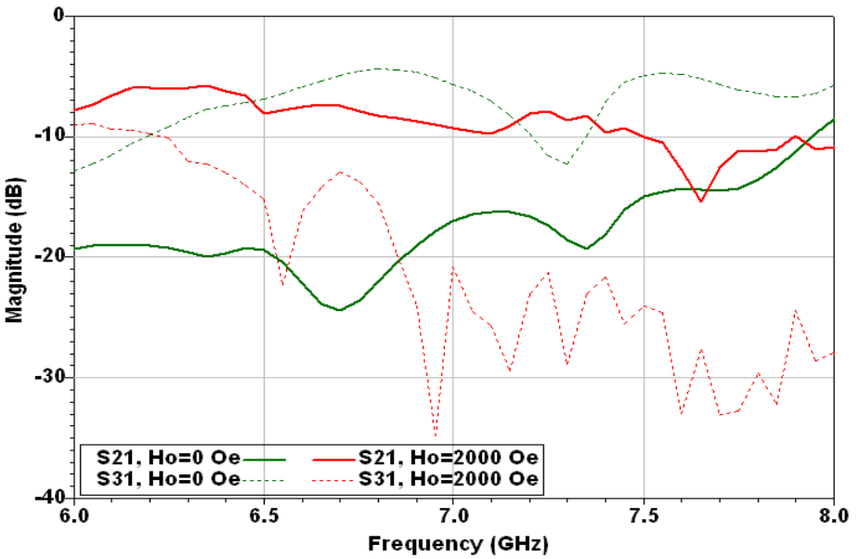

Fig. 18: The measured scattering parameter magnitudes of the dual mode CRLH CPW CLC showing its switching property for H_0=0 Oe and 2000 Oe.

V- Tunable 3 dB CRLH Backward CLC

In this section, we introduce a tunable, CRLH backward CPW CLC implemented on ferrite substrate[66,68]. This coupler was designed to achieve almost power levels for both through and backward coupling, close to 3 dB. The proposed coupler consists of two parallel and identical CRLH CPW TLs. The individual CRLH CPW TLs were designed using shunt planar meandered line inductors and series interdigital capacitors. A conventional ferrite CLC can be tunable, but it requires a longer length which makes it very lossy. Thus, the proposed tunable coupler has the advantages of its compact size and high output levels. Through our proposal 3 dB tunable ferrite CRLH CPW CLC presentation, we introduce its structure, explain the design procedures, and demonstrate the obtained numerical results and the experimental ones for the proposed coupler.

A- Tunable 3 dB CRLH backward CLC structure

The layout diagram of the proposed horizontally magnetized ferrite CRLH CPW CLC is shown in Fig. 19 (a). The CPW CLC was designed using two identical CRLH TLs separated by a distance So. Each CRLH TL was designed by loading the hosting ferrite CPW TL periodically with a shunt meandered line inductor and series interdigital capacitor in two unit cell configurations. For the matching purpose, different configurations of the two interdigital capacitors at input/output ports and the internal capacitor are used. These different configurations are similar to those configurations used in the case of the previous dual mode CLC employing the current dimensions for the tunable 3 dB CRLH CLC. The shunt inductive load is formed by a meandered line inductor with only two meandered arms. The detailed dimensions of the loading elements are shown in Fig. 19 (b and c). Along with loading element value changes, the two lines separation has also increased compared to the previous case to decrease the backward coupling signal level. The loading and parasitic element dimensions were chosen to satisfy the design requirements. Also, the DC magnetic bias direction is reversed compared to the previous case to ensure that the through propagation direction, assuming excitation at port (1), is the same direction as the evanescent propagation direction within the negative ferrite permeability frequency band. Similar to the previously introduced CLC type, the feeding extension CPW TL dimensions at each port of the proposed CPW coupler are identical such that they represent a 50 Ω TL

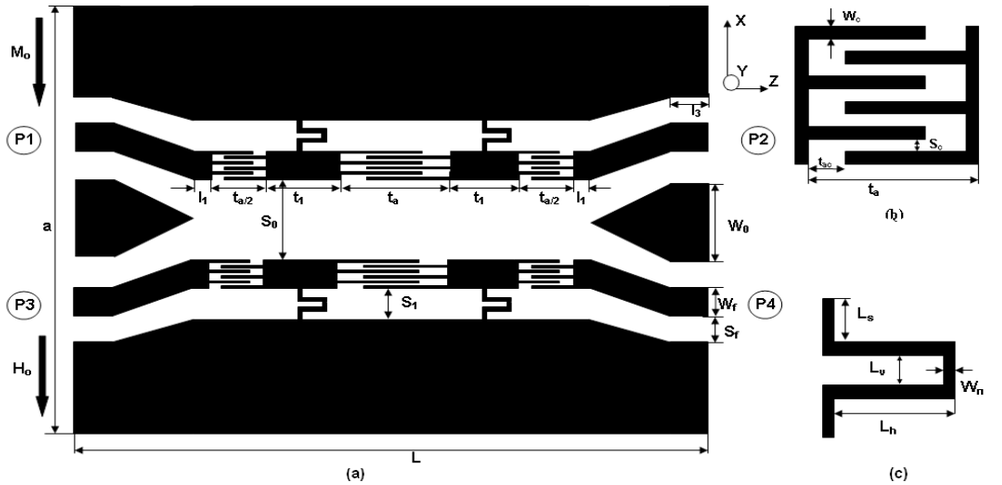

Fig. 19: (a) The layout geometry of the tunable 3 dB ferrite CRLH CPW CLC, a=19.8mm, L=10.32 mm, W_0= 6mm, t_a =2.06 mm, t_1 =1.5mm, l_1 =0.25mm, S_0=2.5mm, S_f=0.8mm, W_f=1.3mm, and l_3=0.1 mm (b) The interdigital capacitor geometry S_c=W_c=0.1mm and t_{ac}=0.4mm (c) The meandered line inductor geometry W_m = 0.25 mm, Ls =0.25 mm, L_v =0.25 mm, and CRLH =0.5 mm[66,68].

B- Tunable 3 dB CRLH backward CLC design procedures

The design procedures of the proposed tunable ferrite 3 dB CRLH backward CLC for different DC magnetic bias values are similar to the procedures followed in the previous case of dual mode CRLH CLC. Consequently, an initially designed 3 dB isotropic CRLH CPW CLC can be obtained by the optimization of the coupler performance using both the circuit modeling and full-wave electromagnetic simulations. The equivalent circuit of the proposed 3 dB CLC can be still illustrated as shown in Fig. 3. Similarly, the initial numerical full wave simulation was carried out assuming a very high DC magnetic bias applied to the ferrite substrate to ensure that it is characterized by its isotropic properties as explained before. Also, similar to the dual mode coupler design introduced before, additional parametric studies for different circuit geometry parameters of the initially designed isotropic CRLH CPW CLC were optimized for different lower DC magnetic bias values. Finally, a tunable almost 3 dB backward CLC can be achieved.

C- Tunable 3 dB CRLH backward CLC numerical results

The scattering parameter magnitudes of the initially proposed coupler designed using HFSS for H_0=50,000 Oe, represent the required very high DC magnetic bias value are shown in Fig. 20. The initial coupler structure has the same dimensions in Fig. 19 except t_a=1.5 mm, t_a=1.8 mm, t_{a0}= 0.2 mm for inner capacitor and 0.05 for outer ones, S_0=2.75 mm, L_s=0.8 mm, and L=10.2 mm. As shown in the figure, the almost equal power levels of both the backward coupling and through signals are quite obvious starting from 4 GHz and extending up to 8 GHz. However, the output levels are not identically equal, but they are enough to start optimization at the desired operating lower DC magnetic bias values as shown next.

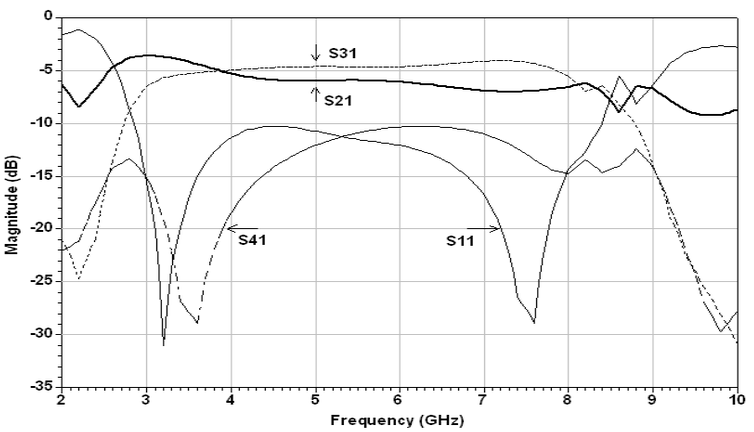

Fig. 20: The full wave simulated scattering parameter magnitudes of the tunable ferrite CRLH CPW CLC for H_0=50,000 Oe.

Then the transmission characteristics of the proposed ferrite CRLH backward CPW CLC were simulated numerically for different DC bias values between 1250 Oe to 2500 Oe to illustrate the tuning capability. The simulated results are shown in Fig. 21. For H_0= 1250 Oe, the simulated scattering parameters are shown in Fig. 21 (a). The coupler has equal through and backward coupling around -4.5 dB, with return loss and coupling isolation better than 20 dB at the center frequency at 3.7 GHz and the coupler's fractional bandwidth is 27 %. The phase difference between the two output signals (S31) and (S21) of the proposed coupler in this case is demonstrating an almost quadrate phase difference within its operating bandwidth with almost 90o at the center frequency, exactly 85°.

For the case of DC magnetic bias equals 1500 Oe, the simulated scattering parameters are illustrated in Fig. 21 (b). In this case, the backward coupling and the through levels are -4 dB and -5 dB respectively with return loss better than 10 dB and coupling isolation better than 20 dB at the center frequency which has been shifted up to 4.05 GHz with the bandwidth increase to 37 %. The phase difference between the two output signals (S31) and (S21) is also demonstrating an almost quadrate phase difference within its operating bandwidth. The phase difference is approximately 75° at the center frequency, whereas approaches 90° near its upper cut-off frequency, at 4.75 GHz.

The simulated scattering parameters for H_0= 1750 Oe are shown in Fig. 21 (c). Both backward coupling and through levels are like the previous case of applying DC magnetic bias of 1500 Oe whereas the isolation level increases more than 25 dB. Similar to the two previous cases, the center frequency and the fractional bandwidth continue increasing by increasing the DC magnetic bias to 4.4 GHz and 54 %, respectively. The phase difference between the two output signals (S31) and (S21) is also demonstrating an almost quadrate phase difference within its operating bandwidth . The phase difference is approximately 81° at the center frequency, whereas approaches exactly 90° near its bandwidth cut-off frequencies, at 3.35 GHz and 5.1 GHz.

By further increasing the DC magnetic bias to 2000 Oe, the simulated scattering parameters are shown in Fig. 21 (d), which illustrates that the center frequency and the fractional bandwidth continue to increase to 4.7 GHz and 55 %, respectively. Also, the phase difference between the two output signals (S31) and (S21) demonstrates almost quadrate phase difference within its operating bandwidth . The such phase difference is approximately 81° at the center frequency, while it approaches exactly 90° near the cut-off frequencies, at 3.35 GHz and 5.5 GHz.

The further studied case for H_0= 2250 Oe is shown in Fig. 21 (e). The coupler demonstrates similar levels for both the backward coupling, the through, and the isolation levels compared with those of the previous case, the 2000 Oe case. However, the through level is a little bit lower starting from 6 GHz. The center frequency in this case is shifted up again to 4.8 GHz where the bandwidth is 60 %. Also, the phase difference between the two output signals (S31) and (S21) demonstrates almost quadrate phase difference within its operating bandwidth. Such phase difference is approximately 81° at the center frequency, while it approaches exactly 90° near its bandwidth upper cut-off frequency, at 6.1 GHz

Finally, H_0 is increased to 2500 Oe where the simulated scattering parameters for this case are shown in Fig. 21 (f). The backward coupling, through, returns loss, and isolation are all close to those of the previous case of 2250 Oe bias, however, the coupled level is increased a little bit. The center frequency and bandwidth have increased even further to 4.9 GHz and 61 %, respectively. Similar to all the above-studied cases, the proposed coupler demonstrates almost quadrate phase difference between its two output signals (S31) and (S21) within its operating bandwidth. The phase difference is approximately 79° the center frequency, while it approaches exactly 90° close to its cut-off frequencies, at 3.4 GHz and 6.5 GHz, respectively.

From the previous results, we can conclude that the proposed CRLH backward CLC has almost equal power levels for both the backward coupling and through output signals with tuning capability for both the center frequency and the bandwidth such that they increase nonlinearly with increasing the applied DC magnetic bias. Also, as predicted in the theoretical analysis, the proposed coupler bandwidth is located within the frequency band of positive permeability of the hosting ferrite CPW TL. This can be confirmed by approximately calculating the onset frequency of negative ferrite permeability using (12). In other words, the cut-off frequencies of the proposed tunable coupler coincide with the onset frequency of negative ferrite permeability. As the onset of the negative ferrite permeability increases with increasing the DC magnetic bias nonlinearly; the center frequency increases with increasing DC bias, showing that the numerical simulations results agree well with the theoretical prediction.

D- Tunable CRLH backward CLC measurement results

The predicted performance of the ferrite tunable coupler has been verified through measurements. The measurement experimental setup and the measurement procedures have been explained previously. Due to the fabrication restriction, the fabricated circuits were based on the commercially available Trans Tech TTVG-1850 as the substrate material. The dimension of this bulk ferrite material is 19 mm x 13 mm x 1 mm. The feeding CPW TL length l3 is increased to 1.5 mm for the sake of SMA connection limitation.

Similar to the previously measured coupler, this current circuit was covered with two horizontal FR4 PCB board covers with 1.5 mm thickness, which were soldered to the SMAs such that the lower cover is 0.6 mm beneath the substrate bottom while the upper cover is 1.9 mm above the printed circuit layout. This fabricated circuit prototype

is shown in Fig. 22 (a). The soldered circuit prototype employing a lower FR4 cover is shown in Fig. 22 (b) whereas, the two-sided circuit prototype is shown in Fig. 22 (c). The horizontal circuit orientation between the two electromagnet poles is similar to the one previously shown in Fig. 10.

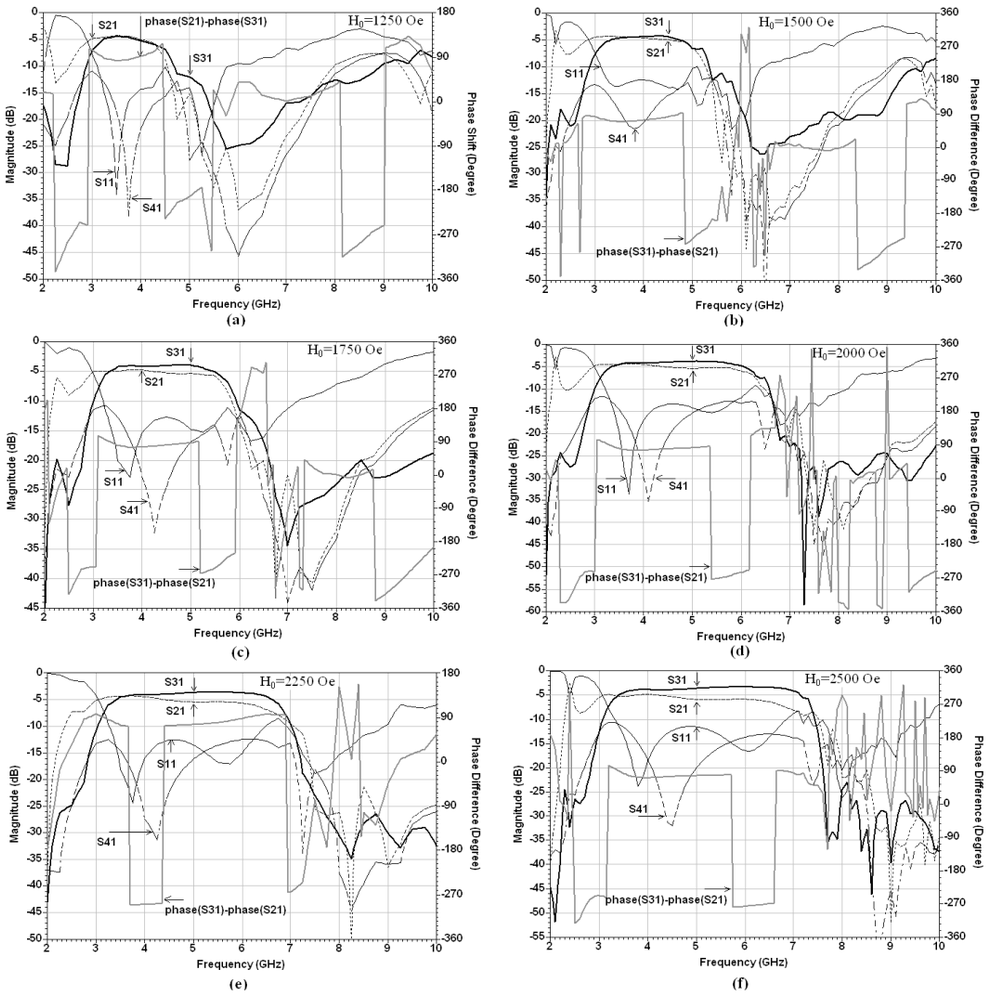

Fig. 21: The full wave simulated magnitudes and phase of scattering parameters of the tunable ferrite CRLH CPW CLC for (a) H_0= 1250 Oe, (b) 1500 Oe, (c) 1750 Oe, (d) 2000 Oe, (e) 2250 Oe, and (f) 2500 Oe.

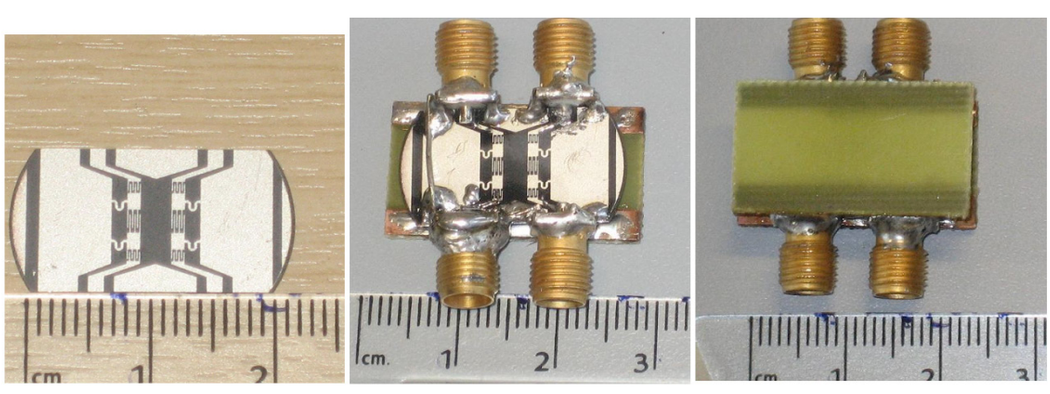

(a) (b) (c)

Fig. 22: The tunable ferrite CRLH CPW CLC made on TTVG-1850 YIG for (a) The circuit prototype (b)

The lower-sided covered circuit prototype (c) The two-sided covered circuit prototype.

During the measurement process, the external field was higher than the internal simulated one by 90 Oe to compensate for the demagnetization field[82].

The measured scattering parameters are shown in Fig. 23 for the same simulated internal DC magnetic values shown in Fig. 21. In the figure it can be observed that the proposed backward coupler operating bandwidth increases by increasing the applied DC magnetic bias. Also, in all cases, the coupler suffers from high reflection within its operating bandwidth resulting in decreasing its two output signal levels compared to the designed one. The high reflection reasons of this coupler circuit are similar to the previous dual mode coupler explained before. Despite the high reflection, the current tunable coupler functionality is still obvious.

In Fig. 23 (a), for H_0=1250 Oe, the coupler demonstrates close levels, not equal, for both the backward coupling and through propagation compared to the forward coupling one. Such levels of both signals are around -10 dB, higher for backward coupling propagation compared to the through one. The coupler bandwidth extends approximately from 2.8 GHz to approximately 4.6 GHz. Within this bandwidth, the through propagation is completely reciprocal. Beyond this frequency band, both signals decay dramatically as a result of the negative ferrite permeability effect. This can be shown clearly by observing a significant nonreciprocal through propagation distinguished by a higher (S12) level compared to (S21) staring from 4.7 GHz and becoming clearer in the frequency band from 5 GHz to 6 GHz. It is worth commenting that the excitation signal for our coupler is at port 1, meaning that no output through propagation exists beyond the previously mentioned coupler bandwidth, 2.8 GHz to 4.6 GHz. The stopband following the coupler bandwidth is characterized by very low output signals, much less than -20 dB. The overlap of the onset frequency of the negative ferrite permeability with the upper cut-off frequency of the coupler bandwidth, for both through and backward coupling signals, confirms the theoretical concepts of this coupler.

For the case of H_0=1500 Oe, its scattering parameters are shown in Fig. 23 (b). The coupler still demonstrates close levels for both the backward coupling and through propagation compared to the forward coupling one within its operating bandwidth. The upper cut-off frequencies of the coupler bandwidth are shifted up to 5 GHz. Also, this frequency coincides with the onset frequency of the negative ferrite permeability which is clearly distinguished by the nonreciprocal through propagation. Within the stopband following the coupler bandwidth, the backward coupled signal decays to less than -20 dB whereas the through signal decays to almost -15 dB up to 5.5 GHz before it continues a rapid decrease to be similar to the backward coupling one.

Similar results for both through and backward coupling signals, within the coupler's operational bandwidth, can be observed by increasing H_0 to 1750 Oe as shown in Fig. 23 (c). Also, the upper cut-off frequency is shifted up again to approximately 5.2 GHz. The through propagation level decreases to below -20 dB before it increases again to be around -12 dB up to 6.4 GHz. In a conclusion, we can comment that both through and backward coupling propagations suffer from a resonance case a little bit higher than 5 GHz. This resonance was not clear in previously studied cases due to dominant evanescent propagation at this frequency due to the effect of the negative ferrite permeability associated with H_0=1250 Oe or 1500 Oe. As a result, the cut-off frequency of the operating bandwidth, in this case, can not be claimed to be 5.2 GHz, but it should be closer to 6.4 GHz.

For H_0=2000 Oe, the measured scattering parameters are shown in Fig. 23 (d). Similar to the previous case, the operating bandwidth of the coupler is extended a little bit to 5. 4 GHz due to the higher onset frequency of the negative ferrite permeability for H_0=2000 Oe. Similar to the previous case, a resonance of the through propagation is clear around 5.5 GHz. This resonance is confirmed by a second increase of the through propagation to be higher than -10 dB from 5.8 GHz to 6.5 GHz before it starts decaying. On the other hand, it can be claimed that the negative ferrite permeability still dominates the resonance nature of the backward coupling signal.

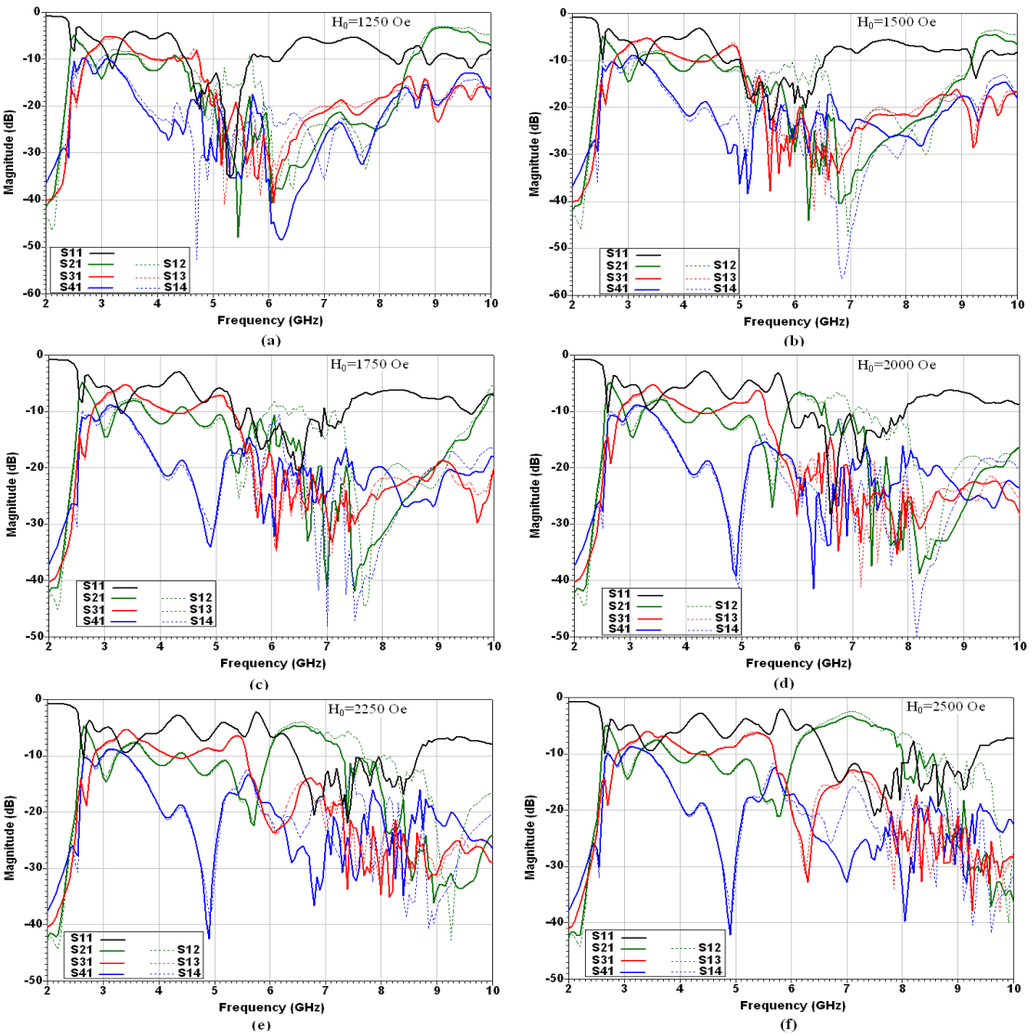

Fig. 23: The measured scattering parameter magnitudes of the tunable ferrite CRLH CPW CLC for(a) H_0= 1250 Oe, (b) 1500 Oe, (c) 1750 Oe, (d) 2000 Oe, (e) 2250 Oe, and (f) 2500 Oe.

The resonance of the backward coupling signal becomes more significant by further increasing H_0 to 2250 Oe and 2500 Oe as in Fig. 23 (e) and Fig. 23 (f), respectively. This resonance can be explained due to the parasitic effects of the measured device configuration. For H_0=2250 Oe, the resonant frequency of the through propagation is clearly around 5.8 GHz after which the through signal increases again to approximately -5 dB within the frequency band from 6 GHz to 7 GHz before it decays due to the negative ferrite permeability. On the other hand, the backward coupling propagation resonant frequency is at 6 GHz and the slow increase of its signal reaches -15 dB within the frequency band from 6.5 GHz to 6.8 GHz before it decays. Also, for H_0=2500 Oe, the resonant frequency of the through propagation is close to the previous case, 5.8 GHz. Following the through signal demonstrate a second passband whose level is -5 dB within the frequency band from 6.2 GHz to 7.8 GHz. The backward coupling propagation has a strong resonance at 6.2 GHz. Then, it increases to approximately -13 dB over the frequency band 6.5 GHz to 7.4 GHz before it is affected by the negative ferrite permeability frequency band.

From all the previous measurement results we can conclude that the measured ferrite coupler is a tunable backward CLC. The cut-off frequency of its operational bandwidth is set up by the onset frequency of the negative ferrite permeability. The levels for its two output signals, the through and the backward coupling, are close but not identically equal. Both output signals have a parasitic resonance which affects their levels and the operating bandwidth; however, it is not significant for DC magnetic bias below 1500 Oe.

By comparing the measurement results with the typically designed structures simulated results shown in Fig. 21 for the same bias values, it can be seen some changes in the output signal levels in addition to the

absence of the parasitic resonance for both output signals in simulated results. The difference between the designed coupler structure and the measured one can be considered as the reason for these variations. To support this theory, the measured structure was numerically simulated using HFSS and its results were compared to the measured ones for the through and backward coupling output signals. This can be shown in Fig. 24, Fig. 25, and Fig. 26 for H_0=1250 Oe, 1750 Oe, and 2250 Oe, respectively.

In general, there is reasonable agreement between the measured and new simulated results from the operation's overall shape point of view. This agreement is very clear at lower DC magnetic bias values and decreases a little by increasing the H_0 value. This can be explained due to the increase of the actual non-uniform DC magnetic field within the ferrite substrate at higher DC magnetic bias values as explained before.

For H_0= 1250 Oe, as shown in Fig. 24, the simulated results for both through and backward coupling propagations are higher than the measured ones by approximately 5 dB within the operating bandwidth. Also, both results can predict the upper cut-off frequency of the coupler bandwidth, especially for the backward coupling case where the two results are almost completely identical. However, the lower cut-off frequency of the through propagation is slightly lower in simulated results compared to measured ones.

More comparison conclusions can be obtained by increasing the DC magnetic bias to 1750 Oe as shown in Fig. 25. Over the starting frequency of the coupler operating bandwidth the signal levels variation is approximately 5 dB. The resonant frequencies for either simulated through or backward coupling signals are higher than the measured ones. The simulated resonant frequency of the backward coupling signal is approximately 6.1 GHz, while it is approximately 5.6 GHz for the measured one. Hence, the simulated results introduce a higher upper cut-off frequency of the coupler bandwidth.

This resonant frequency shift can be clearer by further increasing H0 to 2250 Oe as in Fig. 26. The simulated through resonant frequency is approximately 6.2 GHz while the measured one is 5.6 GHz. Also, the simulated backward coupling signal resonates at 6.8 GHz while it is only 6 GHz in measurement results. Apart from these frequency shifts, the overall shape of the two compared figures is close.

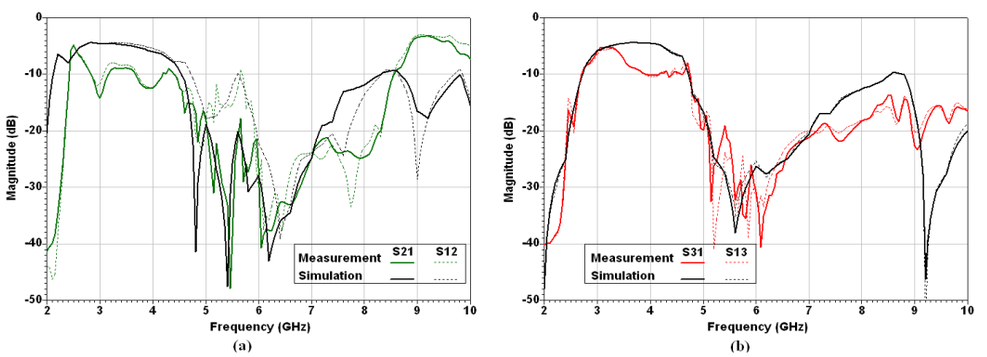

Fig. 24: The comparison between the tunable ferrite CRLH CPW CLC measurement results and the simulation ones for similar measured structure for H_0= 1250 Oe (a) Through comparison (b) Backward coupling comparison.

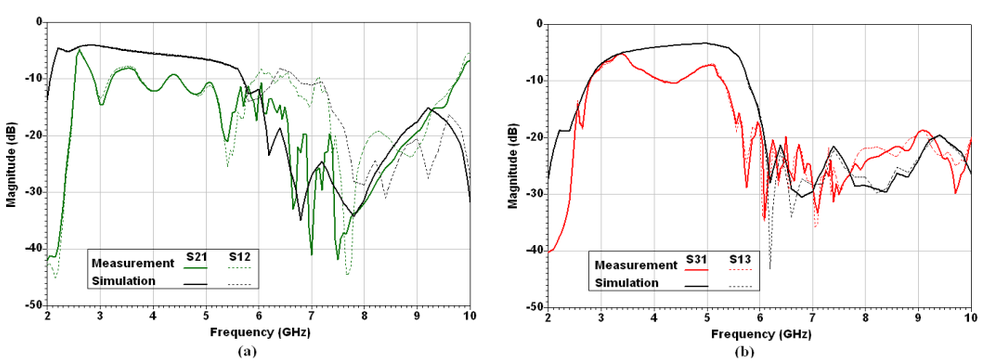

Fig. 25: The comparison between the tunable ferrite CRLH CPW CLC measurement results and the simulation ones for similar measured structure for H0= 1750 Oe (a) Through comparison (b) Backward coupling comparison.

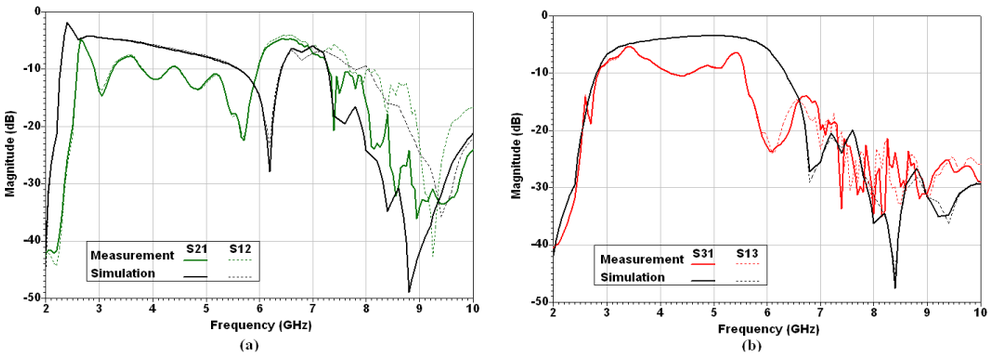

Fig. 26: The comparison between the tunable ferrite CRLH CPW CLC measurement results and the simulation ones for similar measured structure for H_0= 2250 Oe (a) Through comparison (b) Backward coupling comparison.

Finally, a simple and new microwave switch can be introduced as an application of the tunable ferrite CRLH backward CPW CLC. This switching mechanism is based on switching on/off the two output signals by controlling the DC magnetic bias value. As an example to illustrate such a mechanism, the measured scattering parameters of the proposed coupler for H_0=0 Oe are introduced in Fig. 27.

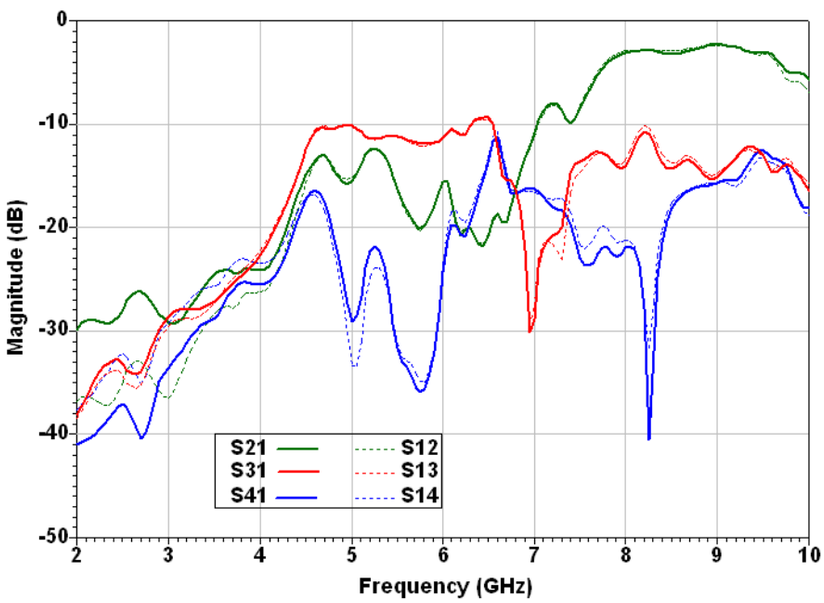

Fig. 27: The measured scattering parameter magnitudes of the tunable ferrite CRLH CPW CLC for H_0=0 Oe.

The backward coupler demonstrates dominant output through and backward coupling signals with levels -10 dB to -15 dB within the frequency band 4.5 GHz to 5.3 GHz. It can be observed that theses two output signals attenuate to -30 dB within the same frequency band in the case of H_0= 1250 Oe in Fig. 23 (a). Thus a novel on/off switch for both through and backward coupling output ports is possible using this coupler by simply changing the DC magnetic bias from 0 Oe to 1250 Oe. This switching mechanism can be considered a completely novel property of the proposed coupler.

In summary, a compact-size tunable ferrite CRLH CPW CLC has been presented. The performance of the coupler has been studied numerically and confirmed by measurements. Both results confirm the tunability of the proposed coupler. Also, a novel microwave on/off switch

is introduced as the application of the proposed coupler.

VI- Compact Nonreciprocal CRLH Forward CLC

It has been explained briefly before that CRLH forward CLC does not need to have a very long physical length and very tight line separation as in the case in conventional forward CLCs. CRLH forward CLC has been introduced using microstrip CRLH TL which achieved approximately 8 dB equal power division for both through and forward coupled ports at 3.6 GHz with more than 80 mm total length[73].

Nonreciprocal forward CLCs can be designed using two long parallel lines over the ferrite substrate. However, the long TLs sections required to achieve a strong forward coupling level will result in high losses of both through and forward coupling due to the lossy nature of the ferrite medium. Forward couplers with nonreciprocal phase properties have been introduced as ferrite-coupled lines (FCL). However, FCL requires a long length and it does not introduce nonreciprocal magnitude properties.

In this section, we introduce a novel compact and nonreciprocal CRLH forward CLC[67]. The proposed coupler was designed in CPW configuration using a ferrite substrate. The proposed CRLH configuration consists of two identical parallel CRLH CPW TLs. Each CRLH TL was designed using a shunt planar strip inductor and series air gap capacitors. The objective of this coupler is mainly to illustrate the nonreciprocal propagation of both the through and forward coupled signal magnitudes at the output terminals.

This novel forward CLC has the advantages of a high forward coupling level, and high nonreciprocity isolation for both two output signals, through and forward coupled, in addition to its compact size and high backward coupling isolation. Also, the proposed coupler can be tunable by changing the applied DC magnetic bias. One of the possible applications of this coupler is the power switching between backward coupling and forward coupling ports which is a novel microwave application introduced here for the first time.

By studying this forward nonreciprocal coupler, we have developed the generalized coupled mode approach for CRLH forward CLC for the first time. Then we modify this approach to be applicable to ferrite CRLH forward CLC. Then we proceed to our proposal coupler to illustrate its structure, explain its design procedures, and introduce the obtained numerical and experimental results.

A- General concepts of CRLH forward coupled line couplers

In our work, we introduce the full wave mathematical solution of a general CRLH forward CLC using the coupled mode approach introduced before for CRLH backward CLC in[80]. This analytical study aims to define mathematical expressions for the coupled line propagation constants and the scattering parameters of a general CRLH forward CLC.

The coupled mode equations for the propagating modes along the two identical left-handed coupled lines can be simplified from equations (1) to (4) assuming backward coupling $C_{BW} = 0$, as

$$\frac{\partial a_1^+}{\partial z} = -j\,\beta_{LH}\,a_1^+ - j\,C_{FW}\,a_2^+ \tag{25}$$

$$\frac{\partial a_2^+}{\partial z} = -j\,\beta_{LH}\,a_2^+ - j\,C_{FW}\,a_1^+ \tag{26}$$

A typical forward coupler is designed such that κm = -κe. In this case, the forward coupling coefficient can be expressed as:

$$C_{FW} = -\frac{L_m}{L_R}\beta_{RH} \tag{27}$$

The coupled propagation constants, βI, II along the CLC can be obtained by solving the above-coupled mode equations assuming a general solution form for these equations as:

$$a_n^+(z) = A_o\, e^{-j\beta z} \tag{28}$$

Where A_o is a general constant while β is the generally coupled mode propagation constant. Substituting from (28) into (25) and (26), the above two coupled mode equations can be expressed in matrix form as:

$$\begin{bmatrix} \beta_{LH}-\beta & C_{FW} \\ C_{FW} & \beta_{LH}-\beta \end{bmatrix} \begin{bmatrix} a_1^+(z) \\ a_2^+(z) \end{bmatrix} = \begin{bmatrix} 0 \\ 0 \end{bmatrix} \tag{29}$$

For a non-trivial solution, the determinant of the above first matrix should be set to zero

$$(\beta_{LH}-\beta)^2 - C_{FW}^2 = 0 \tag{30}$$

Finally, the coupled lines propagation constants, βI, II, along the CLC can be found as:

$$\beta_{I,II} = \beta_{LH} \pm C_{FW} \tag{31}$$

Using the superposition principles, the forward coupled waves propagating on line 1 ($a1^+$) and line 2 ($a2^+$) given from (28) can be expressed as:

$$a_1^+(z) = A\,e^{-j\beta_I z} + B\,e^{-j\beta_{II} z} \tag{32}$$

$$a_1^+(z) = A\,e^{-j\beta_I z} + B\,e^{-j\beta_{II} z} \tag{33}$$

Then, by substitution from (32) into (25), the forward waves propagating on line 2 can be expressed as:

$$a_2^+(z) = A\frac{\beta_I - \beta_{LH}}{C_{FW}} e^{-j\beta I z} + B\frac{\beta_{II} - \beta_{LH}}{C_{FW}} e^{-j\beta II z} \quad (34)$$

By applying matching boundary conditions; i.e. assuming excitation at port (1) and the other ports are matched, then we can write:

$$a_1^+(z=0) = a_o \quad (35)$$

$$a_2^+(z=l) = 0 \quad (36)$$

Where (l) is the coupler length. Consequently, the two constants A and B are found as:

$$A = \frac{a_o(\beta_{II} - \beta_{LH})}{(\beta_I - \beta_{LH}) - (\beta_{II} - \beta_{LH})} \quad (37)$$

$$B = \frac{a_o(\beta_I - \beta_{LH})}{(\beta_I - \beta_{LH}) - (\beta_{II} - \beta_{LH})} \quad (38)$$

Finally, the scattering parameters are found to be:

$$S_{11} = 0 \quad (39)$$

$$S_{21} = \frac{Ae^{-j\beta_I l} + Be^{-j\beta_{II} l}}{A + B} \quad (40)$$

$$S_{31} = 0 \quad (41)$$

$$S_{41} = \frac{A(\beta_I - \beta_{LH})e^{-j\beta I l} + B(\beta_{II} - \beta_{LH})e^{-j\beta II l}}{A(\beta_I - \beta_{LH}) + B(\beta_{II} - \beta_{LH})} \quad (42)$$

This newly developed coupled mode analysis of CRLH forward CLC can reveal the fact that the two propagation constants, $\beta I,II$, as can be observed from (31), are always only real value quantities. This is a contrast to CRLH backward CLC cases in which they may be imaginary values. That means, from (42), a 0 dB forward coupling level is not possible using CRLH CLC configurations. However, the CRLH forward CLC can still introduce length reduction at lower frequencies, compared to RH one, since the CRLH TL electrical length is inversely proportional with frequencies.

B- Ferrite CRLH forward coupled line coupler concepts

It has been explained before in the general CRLH CLC theory section, that a forward CLC requires a negative magnetic coupling coefficient (κm), and its value should be negative equal to κm = -κe for a typical forward mechanism. Also, it has been mentioned earlier, that designing a planar CRLH CLC using a specific ferrite substrate, can demonstrate a negative magnetic coupling coefficient (κm) between the two planar parallel coupled lines within the frequency bandwidth of negative permeability of the hosting individual ferrite TLs.

As a result, a ferrite CRLH CLC can be designed to behave as a typical forward CLC within this frequency band by proper design of the TL elements, the mutual inductance, and capacitance. Accordingly, this forward coupler can demonstrate nonreciprocal and tunable characteristics as a result of the ferrite properties.

C- Compact nonreciprocal CRLH forward CLC structure

The objective of this section is to introduce the structure of the proposed nonreciprocal CRLH forward CLC with almost equal power and tunable propagation features. Coplanar waveguide configuration with ferrite substrate was used in the design.

The layout diagram of the proposed ferrite CRLH CPW CLC is shown in Fig. 28. The CRLH CPW CLC was designed using two identical CRLH TLs of three CRLH unit cells. The two TLs are separated by a distance (So). Each CRLH TL was designed using a CPW TL loaded periodically with a shunt planar segment inductor and series air gap capacitor.

Similar to the previously presented CLCs, extension legs of the two coupled lines are added at each line at each port. The dimensions of the CPW TL at each port of the proposed coupler are identical such that they represent a 50 Ω transmission line.

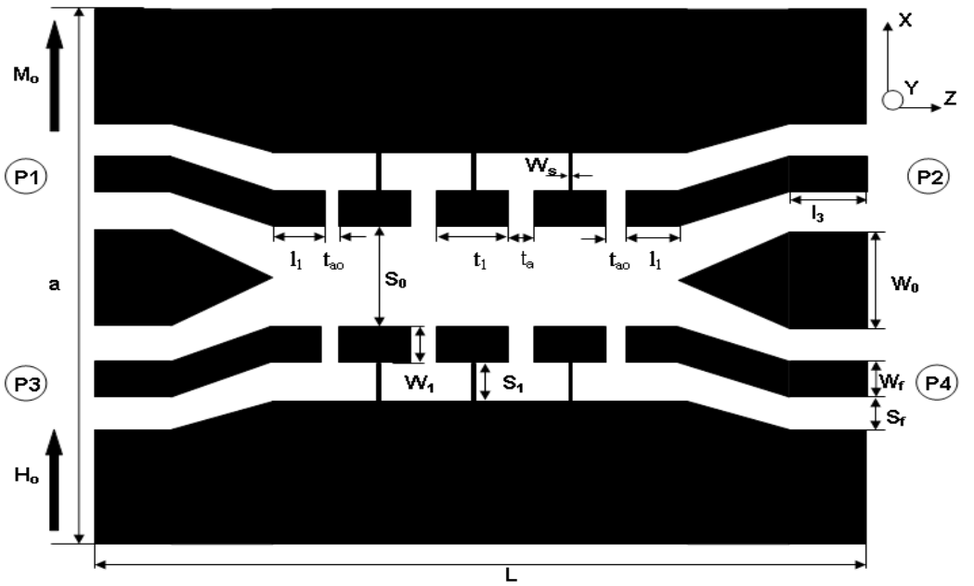

Fig. 28: The layout geometry of the ferrite CRLH forward CPW CLC, a=19.8mm, L=8.6 mm, W_0= 6mm, t_a =0.2 mm, t_{a0} =0.2 mm, t_1 =0.5mm, l_1 =0.1mm, l_3 =1 mm, W_1=0.9 mm, S_1=1.6mm, S_0=0.3 mm, W_s = 0.1 mm, S_f = 0.8mm, and W_f =1.3mm[67].

D- Compact nonreciprocal CRLH forward CLC design procedures

The design objective of the proposed ferrite CRLH forward CPW CLC is to demonstrate nonreciprocal forward coupling with equal power levels. This was fulfilled as explained in the following steps.

The first step is to design a CRLH backward CLC within a specific frequency bandwidth assuming a very high DC magnetic bias is applied to the ferrite substrate. The high DC magnetic bias was selected such that under that bias, the dispersive properties of the hosting ferrite TL are shifted to a very high frequency beyond the lower frequency band of interest. Consequently, the ferrite substrate is characterized by its isotropic properties within the lower frequency band of interest. At this stage, the proposed coupler was designed using the principles of conventional CRLH CLCs assuming two identical coupled individual CRLH transmission lines[80]. Although an optimum CRLH backward coupler performance is not essential in this stage, a high backward coupling level will support the left-handedness of the proposed coupler. "As designed as a backward coupler, the proposed CLC will have a positive magnetic coupling coefficient (κm).

The next step is to select the required DC magnetic bias such that the bandwidth of negative ferrite permeability of the hosting CPW TLs coincides with the specifically designed bandwidth. As explained previously, the proposed coupler demonstrates a backward coupling performance within this frequency bandwidth for high DC magnetic bias. Under that selected lower DC magnetic bias, the individual CRLH TLs are supposed to have a negative magnetic coupling coefficient, κm, which means that the coupling mechanism of the coupler will be no longer backward but forward.

However, a typical forward coupler requires not only a negative magnetic coupling coefficient, κm but also its value should be equal to κm = -κe. Therefore, the final step is optimizing the performance of the proposed coupler under the selected DC magnetic bias to demonstrate the desired typical forward coupler performance. This optimization was done through the parametric studies of the different circuit geometry parameters and the nonreciprocal coupling performance via numerical study.

Moreover, the proposed forward coupler is expected to have a tunable operation by applying different DC magnetic biases. However, not exactly optimum performance of the proposed coupler is expected in these different cases since it operates within the negative ferrite permeability frequency band which is very difficult to model.

E- Compact nonreciprocal CRLH forward CLC numerical results

The proposed coupler structure was simulated for H0= 50,000 Oe representing the desired very high required to ensure that the employed ferrite substrate is characterized only by its isotropic electric properties through the frequency band of interest. The simulated scattering parameters for this case are shown in Fig. 29. At this stage, the dimensions are those given specified in Fig. 28 unless otherwise specified in Fig. 29.

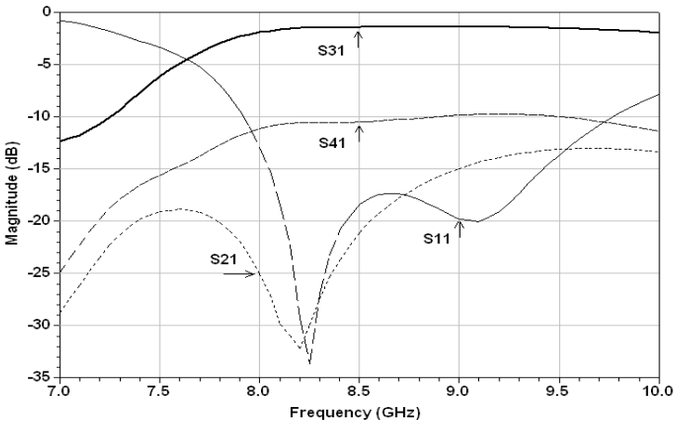

Fig. 29: The full wave simulated scattering parameter magnitudes of the ferrite CRLH forward CPW CLC for H_0= 50,000 Oe, W_1=0.5 mm, t_1 =2 mm, l_1 =0.5mm, l_3=0.5mm, S_0=0.2 mm, and L=11.9mm.

As shown in the above figure, the results show that the coupler under that bias can exhibit a dominant backward coupling propagation in the frequency band starting from a frequency equal to 7 GHz up to almost 9.5 GHz. The backward coupling level is approximately -1 dB over the whole band while the forward coupling level is kept at smaller than or equal to -10 dB. This very high backward coupling level, which can not be achieved using conventional couplers, confirms the designed left-handedness of the proposed coupler. Also, it is noted that the through level is very low within this bandwidth. These data are good enough to start the design of the proposed nonreciprocal forward coupler at a specific DC magnetic bias.

Assuming a lower DC magnetic bias of H0=2500 Oe, the hosting ferrite CPW TL is expected to have a negative permeability within the frequency band approximately from 7 GHz to 9.5 GHz which has been extracted analytically using (12). It is obvious that this bandwidth overlaps with the previously designed almost 0 dB CRLH backward CLC.

The simulated scattering magnitudes of the previously examined coupler for H_0=2500 Oe are shown in Fig. 30. The results show that the previously demonstrated high backward coupling level decreases as the frequency increases, starting with -4 dB at 7 GHz, such that the coupler can be considered not backward coupler starting from 8 GHz up to 10 GHz. The almost -1 dB backward coupling level in the previous case has been changed at a very high decreasing rate to be below -30 dB, between 8.5 GHz to 9.5 GHz. On the other hand, below -10 dB forward coupled level in the previous case has been increased to be around -7 dB within the same frequency bandwidth. Also, the through level has been increased from almost -20 dB in the previous case to around -10 dB level in the current case.

The results confirm that the forward coupling mechanism of the proposed coupler becomes more dominant than the backward one. Also, the switching mechanism from the backward coupling to the forward coupling is very clear within the frequency bandwidth of negative ferrite hosting TL permeability.

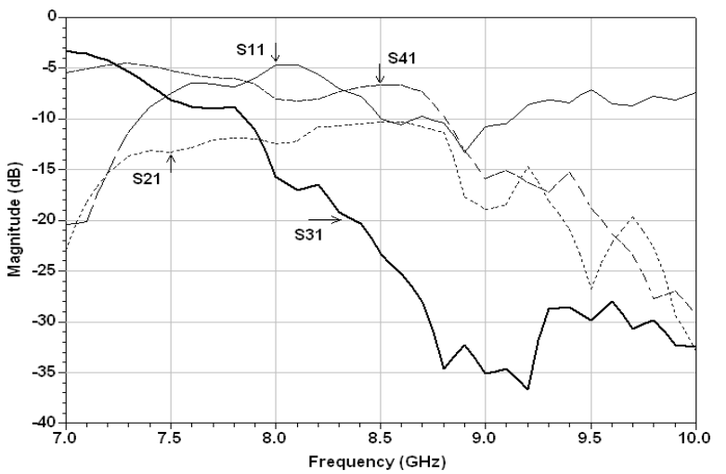

Fig. 30: The full wave simulated scattering parameter magnitudes of the ferrite CRLH forward CPW CLC for H_0= 2500 Oe, W_1=0.5 mm, t_1 =2 mm, l_1 =0.5mm, l_3=0.5mm, S_0=0.2 mm, and L=11.9mm.

A typical forward nonreciprocal performance with specific forward coupling/through signal levels can be achieved through optimization. Thus, for H_0=2500 Oe, many parametric studies of the different circuit geometry parameters aim for optimization of the proposed coupler as a forward nonreciprocal coupling propagation of almost equal power levels for both the two output signals. Finally, the dimensions of the proposed coupler are set to those values specified in Fig. 28 and its simulated magnitudes of the scattering parameters for H_0= 2500 Oe are shown in Fig. 31. As shown in this figure, within the frequency band from 7 GHz to 9 GHz, the levels of both through signal (S21) and forward coupled signal (S41) are equal to be approximately -7 dB. Both the through and forward coupled signals have nonreciprocity propagation with nonreciprocity isolation differences up to 30 dB. Also, the backward coupled signal level of the proposed coupler is quite low with a coupling isolation level of up to 30 dB.

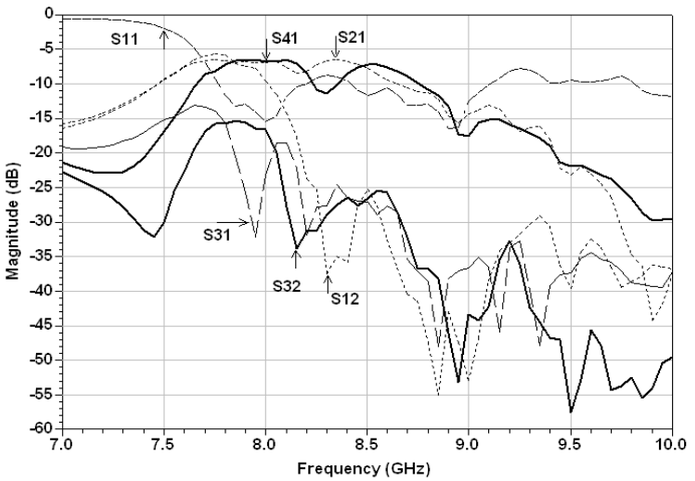

Fig. 31: The full wave simulated scattering parameter magnitudes of the ferrite CRLH forward CPW CLC for H_0=2500 Oe.

It can be observed that the bandwidth of the coupler is typically within the bandwidth of the negative ferrite permeability which can be confirmed mathematically using (12) to be from 7 GHz to 9.3 GHz, approximately. The relative high losses of both propagated signals are because of the lossy nature of the ferrite substrate at the negative ferrite permeability frequency band.

The phase difference between the two output signals is shown in Fig. 32. As shown in the figure, the proposed coupler illustrates almost a quadrate phase shift between the through and the forward coupled signals within the coupler operating bandwidth. However, some discrepancies peaks can be observed at some discrete frequencies. These can be explained since the coupler's bandwidth is within the negative ferrite permeability bandwidth.

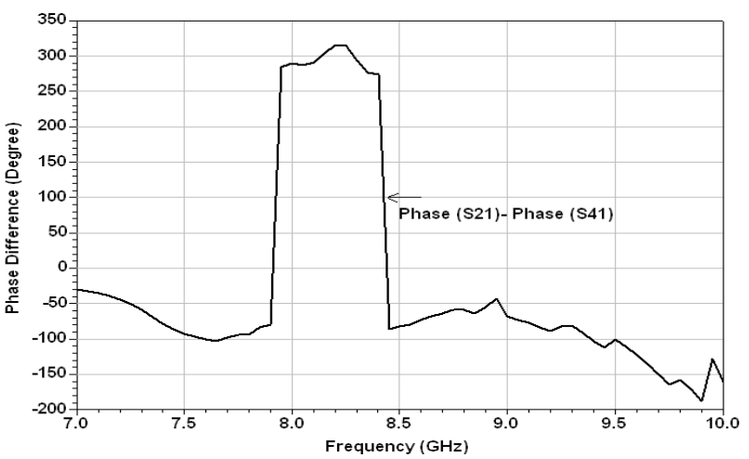

Fig. 32: The full wave simulated phase difference between two output signals of ferrite CRLH forward CPW CLC for H_0=2500 Oe.

To study the tuning capability of the proposed coupler, a lower DC magnetic bias of 2000 Oe was applied and its scattering parameters are shown in Fig. 33. It can be seen that the proposed coupler still has its properties of nonreciprocity for both two output signals but the operating bandwidth is shifted down in frequency to be around 6.75 GHz to 7.5 GHz with obvious lower propagation levels for both outputs signals a little below -10 dB. However, the coupling isolation and nonreciprocal isolation levels are still better than 30 dB within most of the new operating bandwidth. The shift in the operating frequency band can be explained due to the change of the frequency onset of the negative permeability frequency band to be at 5.6 GHz, as calculated from (12). The lower levels of both nonreciprocal output signals, compared to the previous case, can be explained due to the imperfect matching in this new case. This can be seen by increasing the reflection coefficient (S11) level.

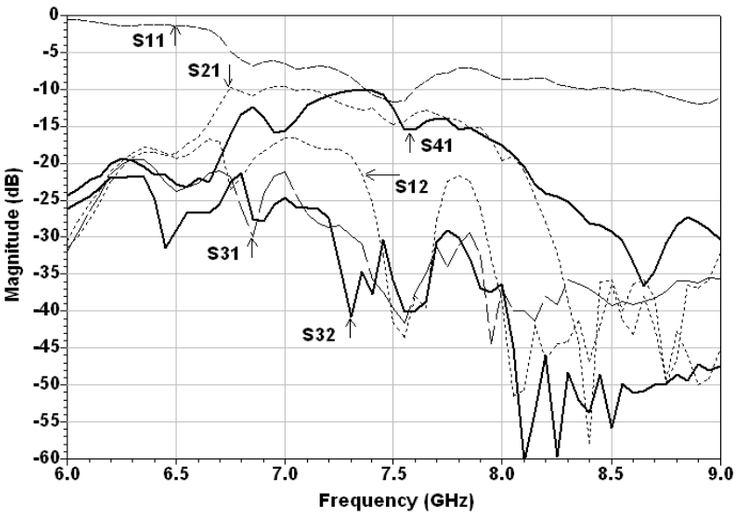

Fig. 33: The full wave simulated scattering parameter magnitudes of the ferrite CRLH forward CPW CLC for H_0=2000 Oe.

F- Compact nonreciprocal CRLH forward CLC experimental results

In this section, we present the measurement results of the proposed CRLH forward coupler. The measured circuit was fabricated on commercially available YIG Trans Tech TTVG-1850 substrate material. The dimension of this bulk material is 19.8 mm x 10.5 mm x 1 mm. The feeding CPW TL length l3 is increased to 2 mm for the simple SMA connection. Similar to all previously measured devices, the proposed coupler was supported with two FR4 PCB covers of 1.5 mm thickness soldered to the SMA connectors at both ends. This fabricated circuit prototype is shown in Fig. 34 (a). The soldered circuit prototype with a lower FR4 cover is shown in Fig. 34 (b) whereas, the two-sided circuit prototype is shown in Fig. 34 (c). The horizontal circuit orientation between the two electromagnet poles is similar to the previously shown in Fig. 10. Approximately 90 Oe increase in the external bias field value was applied to compensate for the demagnetization field[82].

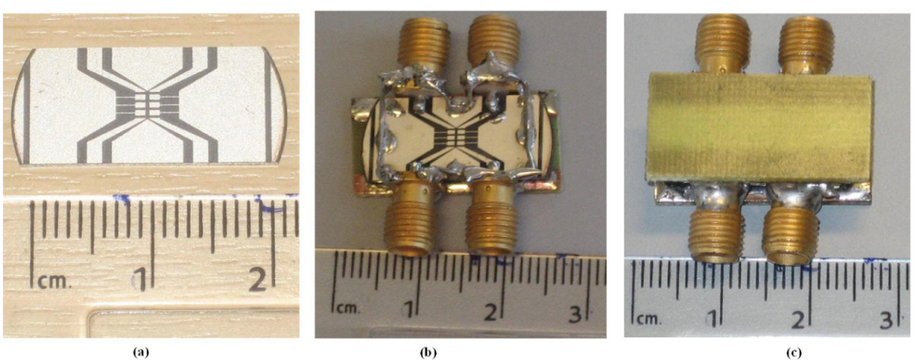

Fig. 34: The fabricated TTVG-1850 ferrite forward CRLH CPW CLC prototype (a) The circuit prototype (b) The lower-sided covered circuit prototype (c) The two-sided covered circuit prototype.

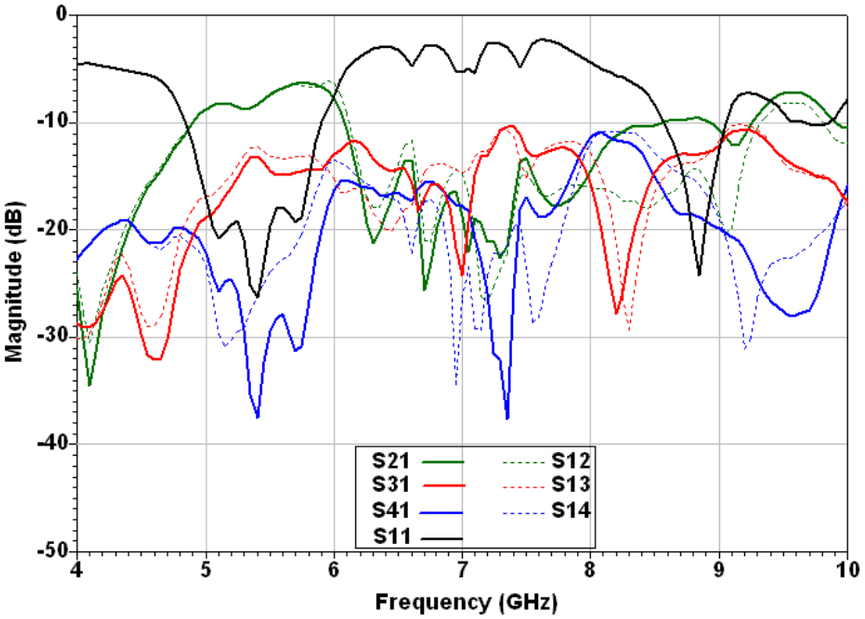

Fig. 35: The measured scattering parameter magnitudes of the ferrite CRLH forward CPW CLC for H_0=0 Oe.

The measured scattering parameters of the forward coupler for H_0=0 Oe are shown in Fig. 35. Similar to previously studied types, this coupler suffers from a high reflection except from 4.8 GHz to 8.5 GHz, approximately, where its level decreases to be around -10 dB. In the figure, the proposed coupler demonstrates dominance through propagation with levels up to -6 dB in the frequency band from 5 GHz to 6 GHz. Within this band, the coupler demonstrates a lower backward coupling level of approximately -15 dB. Also, over the same bandwidth the forward coupling signal is less than -25 dB representing a very high forward coupling isolation level. Following this bandwidth, both the backward coupling signal and forward coupling signal increase while the through decreases within a narrow frequency band from 6 GHz to 6.5 GHz. After this band, from 6.5 GHz to 7 GHz, no significant output signal can be observed. In the narrow frequency bandwidth, 7 GHz to 8 GHz, the backward coupling signal is more dominant whose output signal level is up to -10 dB with more than 10 dB propagation isolation differences for both forward coupling and through. These isolation differences are more significant in the lower bandwidth 7 GHz to 7.5 GHz. Adjacent to this backward coupling bandwidth, a narrow bandwidth from 8 GHz to 8.5 GHz is characterized by approximately -10 dB level for both through and forward coupling signals while the backward coupling signal level decreases to almost -30 dB. Following this narrow bandwidth, the output signals change to be the through signal and backward coupling signal with different levels. Then, both signals decay considerably at 10 GHz.

By closely looking at the measurement results of the coupler for H_0 = 0 Oe, it can be observed the followings. First, the ferrite substrate is considered almost isotropic within the whole studied bandwidth, 4 GHz to 10 GHz. Second, the ferrite CRLH CLC can demonstrate backward coupling within the frequency band of 7 GHz to 7.5 GHz. Within this bandwidth, as mentioned above, the backward coupling level is -10 dB while both the through and forward coupling levels are below -20 dB.

As explained in the design procedures section of the proposed forward ferrite CLC, a ferrite CRLH backward CLC can be designed to demonstrate forward coupling instead of the backward one by applying DC magnetic bias inducing negative ferrite permeability within the backward coupling bandwidth. Consequently, by applying DC magnetic bias of H_0 around 2500 Oe, it is expected that the coupler can behave as a nonreciprocal forward coupler within, or very close to, that bandwidth. Thus, the scattering parameters of the proposed coupler were measured and plotted in Fig. 36 for H_0=2500 Oe where it can be observed a high reflection level of approximately -10 dB over the whole bandwidth. Similar to all previous types, such high reflection can be explained due to the circuit measurement configuration.

It can be noted that no backward propagation is dominant over the whole bandwidth from 7 GHz to 10 GHz. Within this frequency band, the backward coupling level is below -20 dB. By comparing this behavior to the backward coupling level in Fig. 35, we observe that the coupler demonstrates at least a 10 dB decreases in its backward coupling level. This is more significant within the frequency band 7 GHz to 7.5 GHz within which the level decreases almost from -10 dB to -25 dB. On the other hand, it is observed the increase of both the through and

forward coupling propagations within the frequency band from 7 GHz to 8.25 GHz. Specifically, within the frequency band 7.7 GHz to 8.1 GHz, it can be observed a narrow bandwidth characterized by almost equal power levels for both nonreciprocal forward coupling and through signals. The levels of the two signals are very close to -10 dB within this bandwidth. Moreover, both signals have significant nonreciprocal properties with a nonreciprocity isolation difference of more than 10 dB within this bandwidth.

Finally, we can say that the proposed measured device acts to some acceptable level as a nonreciprocal forward CLC within the frequency bandwidth from 7.7 GHz to 8.1 GHz with more than 10 dB backward coupling isolation and nonreciprocity isolation differences. By comparing these results to the originally designed ones shown in Fig. 31, significant variations have been observed for both the forward coupling operating bandwidth and its output levels. However, the same concept of the possibility of achieving a nonreciprocal forward CLC is confirmed by measurement results.

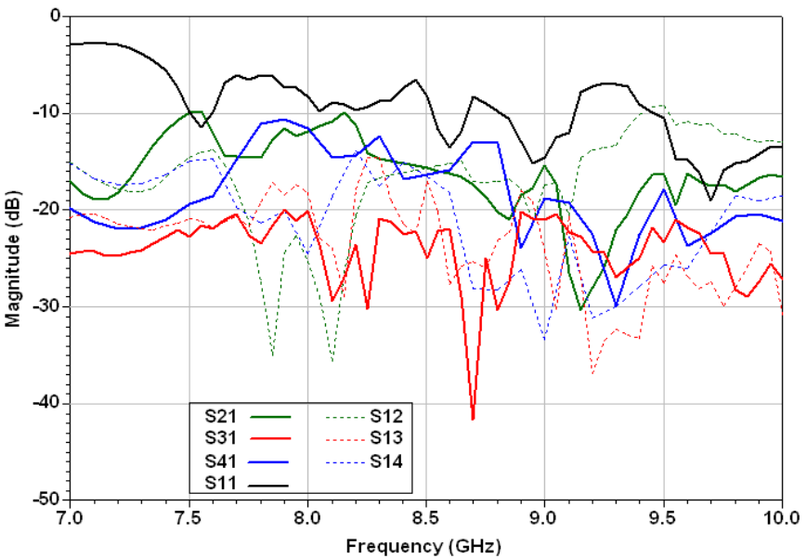

Fig. 36: The measured scattering parameter magnitudes of the ferrite CRLH forward CPW CLC for H_0=2500 Oe.

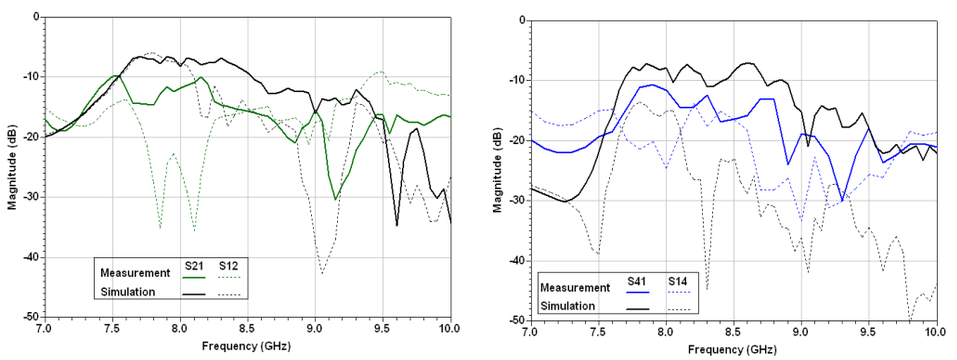

Fig. 37: The comparison between the ferrite CRLH forward CPW CLC measurement results and the simulation ones for similar measured structures for H0= 2500 Oe (a) Through comparison (b) Forward coupling comparison.

To analyze the differences between the designed device and the measured one, we simulated the same measured structure using HFSS. The new simulated results are compared to the measured ones for both the through and the forward coupling signals as shown in Fig. 37. The through-signal propagation comparison is shown in Fig. 37 (a). Can observe a good agreement between the two results on the thorough propagation within the frequency band 7 GHz to 7.5 GHz. The simulated results show an almost flat signal whose level is approximately -7 dB in the frequency

band from 7.65 GHz to 8.3 GHz. Also, it starts to have nonreciprocal properties from 8 GHz. On the other hand, the measured through-level is significantly lower than the simulated one; it is 3 dB below and reaches 10 dB in the worst case. Moreover, the nonreciprocity properties of the measured through-level results start at 7.7 GHz, lower than the simulated one by approximately 0.3 GHz. Above 8.5 GHz, both measured and simulated results start decaying. Although the decaying signal levels are different in the two cases, the physical phenomenon can be observed.

Similar results can be observed by comparing the measured and simulated forward coupling signals as shown in Fig. 37 (b). Both results show the onset of the forward coupling propagation growing up at 7.55 GHz. The simulated forward coupling signal shows an almost flat signal in the frequency band 7.7 GHz to 8.65 GHz, except for some small decreasing steps at 8.05 GHz and 8.3 GHz. Also, this propagation is nonreciprocal over that bandwidth. The measured forward coupling signal shows a good agreement with the simulated one in the frequency band from 7.7 GHz to 8 GHz, only its level is lower by no more than 3 dB. The nonreciprocity properties of the measured results agree with the simulated ones in the lower frequencies from 7.7 GHz to 8.1 GHz, considering the reasonable difference between the two compared signal levels in this frequency band.

In general, we can say that these two comparisons have given reasonably accepted phenomenon verification. However, some variations between the measured and simulated results are not small. These variations can be explained due to the strong effect of the actual non-uniform DC magnetic field within the ferrite substrate while it was assumed uniform in the simulation results. This effect was noticed to be strong at high DC magnetic bias values as reported in the previously measured devices. This effect should be considered in the evaluation of the comparison. Also, some of these variations may be explained since the coupler's operating bandwidth is within the negative ferrite permeability which is very difficult to model the device performance within it. Also, the inaccurate variations in behavior can be due to the resonances introduced by the measured device configuration. The measurement results in Fig. 36 further confirm the theoretical prediction that a dominant backward coupling of a ferrite CRLH CLC can be switched to either forward coupled or through ports.

The switching mechanism of the proposed coupler from the backward coupling mechanism to the forward coupling one can be further confirmed by giving more focus on the frequency band from 5 GHz to 6 GHz. Within this frequency band for the case of H_0=0 Oe shown in Fig. 35, the ferrite CRLH CLC can be claimed to have a backward coupling mechanism, not the ideal one. The backward coupling signal level within this band increases from -18 dB at 5 GHz to -12 dB at 6 GHz. On the other hand, the forward coupling signal level is approximately less than -25 dB over most of this bandwidth. Also, the through propagation is the main output signal of the coupler with a level of around -7 dB over this bandwidth.

For H_0 within the range from 1500 Oe to 1750 Oe, it is expected that the individual hosting ferrite TLs have a negative permeability within that frequency band. Consequently, the performance of the proposed coupler was measured using its scattering parameters for H_0=1500 Oe and 1750 Oe as shown in Fig. 38 and Fig. 40, respectively. In the two figures, we can observe a high reflection coefficient which will affect results by decreasing the output signal levels in each case. But, the switching mechanism can be still noted by observing the dominant signal level in each case as explained in the following.

For the case of H_0=1500 Oe, it can be observed that the through signal is affected by the losses of the ferrite substrate within its negative ferrite permeability bandwidth. This is clear as it is a level decrease starting from 4.5 GHz, compared to Fig. 35. However, the through propagation is still the dominant propagation of the ferrite CRLH CLC. Then, by focusing on the backward coupling signal behavior, we observe that its level is approximately around -25 dB in the frequency band from 4.5 GHz to 6 GHz, apart from a single resonance peak of -18 dB at 5.5 GHz. On the other hand, the forward coupling signal level increases to approximately -16 dB within the frequency band 5.2 GHz to 5.7 GHz, apart from a small resonance at 5.55 GHz. As a summary, we can say that the forward coupling signal level increases at the expense of the backward coupling signal, with an average of 10 dB. Thus, it can be claimed that within the negative ferrite permeability frequency band, the proposed coupler changes its coupling mechanism to be switched from backward coupling to forward one. This switching mechanism is made clearer in Fig. 39.

The previous example for H_0 = 1500 Oe suffers from many resonances that may cause the proposed switching mechanism not to be clear. This switching mechanism can be clearer for H_0 = 1750 Oe shown in Fig. 40. In the figure, it is so obvious that the forward coupling signal level increase from -20 dB at 5.5 GHz to approximately -12 dB at 6 GHz. Within this bandwidth, the backward signal level is between -20 dB to -30 dB. By comparing these levels to their corresponding in Fig. 35, we can observe that the forward coupling signal acquires at least a 10 dB increase in its level while the backward coupling signal level suffers more than a 15 dB decrease. This switching mechanism is made clearer in Fig. 41.

From the two studied cases, we can confirm that the switching mechanism is possible within the negative ferrite permeability bandwidth. However, this switching mechanism might not guarantee a switch between a typical backward coupler to a typical forward coupler since the forward coupler should be designed through circuit parameters optimization at a specific DC magnetic bias value like the one designed for H_0=2500 Oe. Finally, we can claim that the measurement results confirmed the performance of this coupler as a nonreciprocal forward CLC within the negative ferrite permeability frequency band. This proves the theoretical prediction of the

possibility of designing a nonreciprocal forward CLC within that bandwidth.

In summary, nonreciprocal forward CRLH CPW CLCs on a ferrite substrate have been presented. The general CRLH forward coupler theory has been developed. The theoretical analysis of the proposed coupler has been given and validated numerically and experimentally. The results show that a compact CRLH forward CLC can be achieved. Also, a switching coupling mechanism is introduced

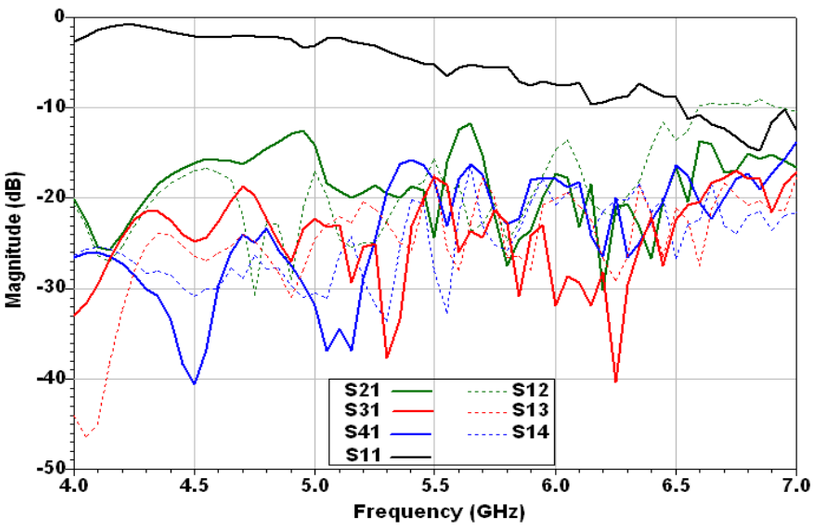

Fig. 38: The measured scattering parameter magnitudes of the ferrite CRLH forward CPW CLC for H_0=1500 Oe

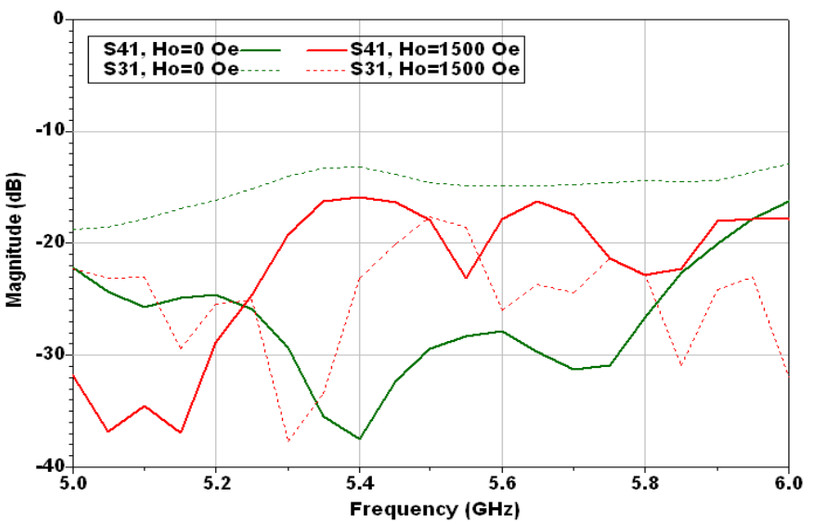

Fig. 39: The measured scattering parameter magnitudes of the CRLH forward CPW CLC show its switching property for H_0=0 Oe and 1500 Oe

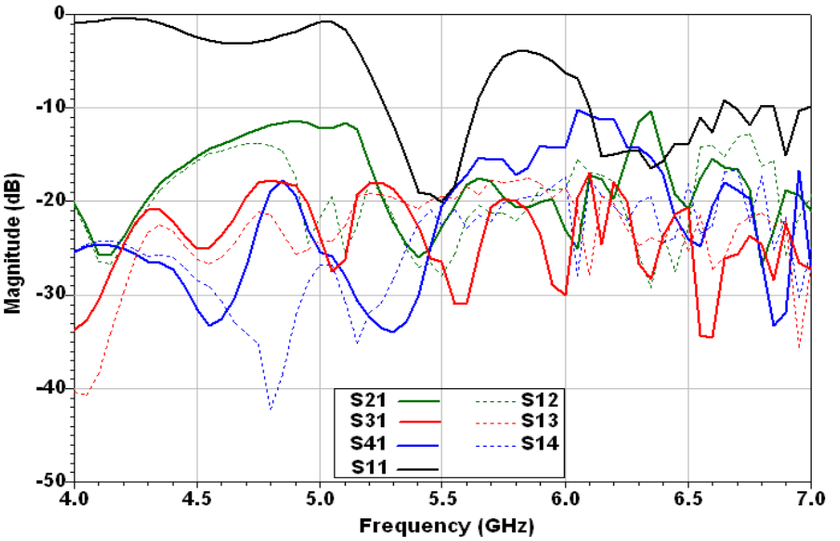

Fig. 40: The measured scattering parameter magnitudes of the ferrite CRLH forward CPW CLC for H_0=1750 Oe.

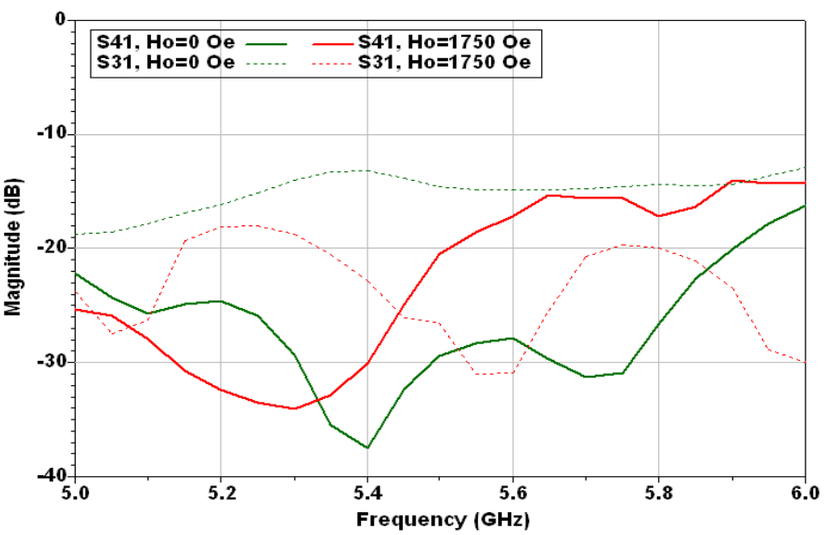

Fig. 41: The measured scattering parameter magnitudes of the CRLH forward CPW CLC showing its switching property for H_0=0 Oe and 1750

VII- Conclusion

Different novel types of ferrites CRLH CPW CLCs, comprising backward and forward couplers with different propagation levels have been designed, fabricated, measured, and characterized. All couplers were designed using two separated and parallel identical CRLH TLs over a horizontally magnetized ferrite substrate. Different loading element configurations are employed in designing individual CRLH TLs according to their corresponding coupler's desired function. All couplers have the advantages of compact size and small demagnetization factors. In addition, all proposed ferrite CRLH CLCs here can demonstrate tunability and/or nonreciprocity properties.

Based on the CRLH symmetrical backward CLC theory, the general ferrite CRLH CLC concepts have been introduced to backward CLCs with ferrite medium properties. Theoretical analysis illustrates that a ferrite CLC demonstrate a backward coupling mechanism within the frequency band characterized by positive ferrite permeability. Within the negative permeability bandwidth backward coupling is not exist. However forward coupling can be designed to demonstrate the nonreciprocal combination of through and forward coupling performance. The theoretical analytical design, numerical design results, and experimental measurement results are presented for

each coupler. The measurement and numerical results confirm the couplers' functionalities with some explained level variations.

The first introduced coupler is a dual mode (band) nonreciprocal ferrite CRLH CPW backward CLC. The results show that the first coupler band is reciprocal backward propagation and it requires a positive relative permeability of the hosting ferrite CPW TL. The second band is nonreciprocal through one which requires negative ferrite permeability. This coupler can be considered a unique coupler which can not be achieved using any coupler type. The power switching mechanism between the two bands can be achieved according to the applied DC magnetic bias.

The second proposed coupler is a single-band compact tunable ferrite CRLH backward CPW CLC. Within its operating bandwidth, equal power levels for the backward coupling and through propagation are designed. This coupler has the advantages of its compact size and its high output signal levels compared to ferrite CLC. This proposed coupler can be utilized as a microwave on/off switch.

Finally, a novel nonreciprocal ferrite CRLH forward CPW CLC has been introduced. The proposed coupler operates within the negative ferrite permeability frequency band of the individuals hosting ferrite TLs. The proposed coupler represents a good example of the backward coupling mechanism switching which may be applied in novel microwave switching applications.

6. References

[1] 1. S.-G. Mao, S.-L. Chen, and C.-W. Huang, "Effective electromagnetic parameters of novel distributed left-handed microstrip lines," IEEE Transactions on Microwave Theory and Techniques, vol. 53, pp. 1515-1521, 2005.
[2] F. Falcone, T. Lopetegi, J. D. Baena, R. Marques, F. Martin, and M. Sorolla, "Effective negative-ε stopband microstrip lines based on complementary split ring resonators," IEEE Microwave and Wireless Components Letters, vol. 14, pp. 280-282, 2004.
[3] F. Falcone, F. Martin, J. Bonache, R. Marques, T. Lopetegi, and M. Sorolla, "Left handed coplanar waveguide band pass filters based on bi-layer split ring resonators," IEEE Microwave and Wireless Components Letters, vol. 14, pp. 10-12, 2004.
[4] Jordi Naqui, Miguel Duran-Sindreu, Armando Fernandez-Prieto, Francisco Mesa, Francisco Medina, and Ferran Martin. "Multimode propagation and complex waves in CSRR-based transmission-line metamaterials." IEEE Antennas and Wireless Propagation Letters, vol. 11, pp. 1024-1027, 2012.
[5] Lijuan Su, Jordi Naqui, Javier Mata-Contreras, and Ferran Martín. "Modeling and applications of metamaterial transmission lines loaded with pairs of coupled complementary split-ring resonators (CSRRs)." IEEE Antennas and Wireless Propagation Letters, vol. 15, pp.154-157, 2015.
[6] G. V. Eleftheriades, A. K. Iyer, and P. C. Kremer, "Planar negative refractive index media using periodically L-C loaded transmission lines," IEEE Transactions on Microwave Theory and Techniques, vol. 50, pp. 2702-2712, 2002.
[7] C. Caloz and T. Itoh, "Transmission line approach of left-handed (LH) materials and microstrip implementation of an artificial LH transmission line," IEEE Transactions on Antennas and Propagation, vol. 52, pp. 1159-66, 2004.
[8] C. Caloz "Metamaterial dispersion engineering concepts and applications." Proceedings of the IEEE, vol. 99, no. 10, pp. 1711-1719, 2011.
[9] C. Caloz and T. Itoh, Electromagnetic metamaterials transmission line theory and microwave applications. New jersey: John Wiey & Sons, 2006.
[10] O. F. Siddiqui, M. Mojahedi, and G. V. Eleftheriades, "Periodically loaded transmission line with effective negative refractive index and negative group velocity," IEEE Transactions on Antennas and Propagation, vol. 51, pp. 2619-25, 2003.
[11] A. Sanada, C. Caloz, and T. Itoh, "Characteristics of the composite right/left-handed transmission lines," IEEE Microwave and Wireless Components Letters, vol. 14, pp. 68-70, 2004.
[12] A. Grbic and G. V. Eleftheriades, "Periodic analysis of a 2-D negative refractive index transmission line structure," IEEE Transactions on Antennas and Propagation, vol. 51, pp. 2604-11, 2003.
[13] A. Sanada, C. Caloz, and T. Itoh, "Planar distributed structures with negative refractive index," IEEE Transactions on Microwave Theory and Techniques, vol. 52, pp. 1252-63, 2004.
[14] Ayman H. Dorrah, and George V. Eleftheriades. "Pencil-beam single-point-fed Dirac leaky-wave antenna on a transmission-line grid." IEEE Antennas and Wireless Propagation Letters, vol. 16, pp. 545-548, 2016.
[15] Jiahao Zhang, Sen Yan, and Guy AE Vandenbosch. "A Multistandard Antenna Based on a 2-D CRLH-TL in Polar Coordinates." IEEE Antennas and Wireless Propagation Letters, vol. 20, no. 3, pp. 332-336, 2021.
[16] J. Yamauchi, Ueda, T. Kubo, Y., and, T. Itoh, "Enhancement of phase-shifting nonreciprocity in microstrip-line-based metamaterials by using a combination of their curvatures and asymmetrical insertion of stubs". IEEE Transactions on Microwave Theory and Techniques, vol. 65, no. 12, pp. 5123-5132, 2017.
[17] Sarkar, Anirban, Duc Anh Pham, and Sungjoon Lim. "Tunable higher order mode-based dual-beam CRLH microstrip leaky-wave antenna for V-band backward–broadside–forward radiation coverage." IEEE Transactions on Antennas and Propagation, vol. 68, no. 10, pp. 6912-6922, 2020.
[18] S.-G. Mao, M.-S. Wu, Y.-Z. Chueh, and C. H. Chen, "Modeling of symmetric composite right/left-handed coplanar waveguides with applications to compact bandpass filters," IEEE Transactions on Microwave Theory and Techniques, vol. 53, pp. 3460-6, 2005.
[19] J. Gao and L. Zhu, "Characterization of infinite- and finite-extent coplanar waveguide metamaterials with varied left- and right-handed passbands," IEEE Microwave and Wireless Components Letters, vol. 15, pp. 805-7, 2005.
[20] Shih-Chia Chiu, Chien-Pai Lai, and Shih-Yuan Chen. "Compact CRLH CPW antennas using novel termination circuits for dual-band operation at zeroth-order series and shunt resonances." IEEE transactions on antennas and propagation, vol. 61, no. 3, pp. 1071-1080, 2012.
[21] Pei-Ling Chi, and Yi-Sen Shih. "Compact and bandwidth-enhanced zeroth-order resonant antenna." IEEE Antennas and Wireless Propagation Letters, vol 14, pp. 285-288, 2014.
[22] Mohamed AG Elsheikh, Nancy Y. Ammar, and Amr ME Safwat. "Analysis and design guidelines for wideband CRLH SRR-loaded coplanar waveguide." IEEE Transactions on Microwave Theory and Techniques 68, no. 7, pp. 2562-2570, 2020.
[23] Mohamed El Atrash, Mahmoud A. Abdalla, Hadia M. Elhennawy, "A Compact Highly Efficient Π-Section CRLH Antenna loaded with Textile AMC for Wireless Body Area Network Applications", IEEE Transactions on Antennas and Propagation, vol. 69, no. 2, pp. 648 - 657, Feb. 2021.
[24] Vélez, Paris, Miguel Durán-Sindreu, Armando Fernández-Prieto, Jordi Bonache, Francisco Medina, and Ferran Martı. "Compact dual-band differential power splitter with common-mode suppression and filtering capability based on differential-mode composite right/left-handed transmission-line metamaterials." IEEE Antennas and Wireless Propagation Letters, vol. 13, pp. 536-539, 2014.
[25] Liu, Fu-Xing, and Jong-Chul Lee. "A Dual-Mode Power Divider With Embedded Meta-Materials and Additional Grounded Resistors." IEEE Transactions on Microwave Theory and Techniques, vol. 69, no. 8, pp. 3607-3615, 2021.
[26] Huang, Taotao, Linping Feng, Li Geng, Haiwen Liu, Shao Yong Zheng, Sheng Ye, Lina Zhang, and Hao Xu. "Compact Dual-Band Wilkinson Power Divider Design Using Via-Free D-CRLH Resonators for Beidou Navigation Satellite System." IEEE Transactions on Circuits and Systems II: Express Briefs, vol. 69, no. 1, pp. 65-69, 2021.
[27] Liu, Fu-Xing, Yang Wang, Shi-Peng Zhang, and Jong-Chul Lee. "Design of compact tri-band Gysel power divider with zero-degree composite right-/left-hand transmission lines." IEEE Access, vol. 7, pp. 34964-34972, 2019

[28] Ren, Xue, Kaijun Song, Maoyu Fan, Yu Zhu, and Bingkun Hu. "Compact dual-band Gysel power divider based on composite right- and left-handed transmission lines." IEEE Microwave and Wireless Components Letters, vol. 25, no. 2, pp. 82-84, 2014.
[29] Chi, Pei-Ling, and Tse-Yu Chen. "Dual-band ring coupler based on the composite right/left-handed folded substrate-integrated waveguide." IEEE microwave and wireless components letters, vol. 24, no. 5, pp. 330-332, 2014.
[30] Chang, Li, and Tzyh-Ghuang Ma. "Dual-mode branch-line/rat-race coupler using composite right-/left-handed lines." IEEE Microwave and Wireless Components Letters, vol. 27, no. 5, pp. 449-451, 2017.
[31] M. A. Abdalla, M. A. Fouad, H. A. Elregeily, and A. A. Mitkees, "Wideband Negative Permittivity Metamaterial for size reduction of stopband filter in Antenna Applications", Progress In Electromagnetics Research C, vol. 25, pp. 55-66, 2012.
[32] Mohan, Manoj Prabhakar, Arokiaswami Alphones, and M. F. Karim. "Triple band filter based on double periodic CRLH resonator." IEEE Microwave and Wireless Components Letters, vol. 28, no. 3, pp. 212-214, 2018.
[33] Song, Yi, Pin Wen, Haiwen Liu, Yifan Wang, and Li Geng. "Design of compact balanced-to-balanced diplexer using dual-mode CRLH resonator for RFID and 5G applications." IEEE Journal of Radio Frequency Identification, vol. 3, no. 3, pp. 143-148, 2019.
[34] Song, Yi, Haiwen Liu, Weilong Zhao, Pin Wen, and Zhengbiao Wang. "Compact balanced dual-band bandpass filter with high common-mode suppression using planar via-free CRLH resonator." IEEE Microwave and Wireless Components Letters, vol. 28, no. 11, pp. 996-998, 2018.
[35] Shen, Guangxu, Wenquan Che, Quan Xue, and Wanchen Yang. "Characteristics of dual composite right/left-handed unit cell and its applications to bandpass filter design." IEEE Transactions on Circuits and Systems II: Express Briefs, vol. 65, no. 6, pp. 719-723, 2017.
[36] Shen, Guangxu, Wenquan Che, Quan Xue, and Wenjie Feng. "Novel design of miniaturized filtering power dividers using dual-composite right-/left-handed resonators." IEEE Transactions on Microwave Theory and Techniques, vol. 66, no. 12, pp. 5260-5271, 2018.
[37] Guan, Xuehui, Hui Su, Haiwen Liu, Pin Wen, Wang Liu, Ping Gui, and Baoping Ren. "Miniaturized high temperature superconducting bandpass filter based on D-CRLH resonators." IEEE Transactions on Applied Superconductivity, vol. 29, no. 5, pp. 1-4, 2019.
[38] Wang, Zhan, Yinwan Ning, and Yuandan Dong. "Hybrid Metamaterial-TL Based, Low-Profile, Dual-Polarized Omnidirectional Antenna for 5G Indoor Application." IEEE Transactions on Antennas and Propagation, Vol. 70, no. 4, pp. 2561 - 2570, April 2022.
[39] Wang, Zhan, Tian Liang, and Yuandan Dong. "Composite Right-/Left-Handed-Based, Compact, Low-Profile, and Multifunctional Antennas for 5G Applications." IEEE Transactions on Antennas and Propagation, vol. 69, no. 10, pp. 6302-6311, 2021.
[40] Huang, Taotao, Linping Feng, Li Geng, Haiwen Liu, Shao Yong Zheng, Sheng Ye, Lina Zhang, and Hao Xu. "Compact Dual-Band Wilkinson Power Divider Design Using Via-Free D-CRLH Resonators for Beidou Navigation Satellite System." IEEE Transactions on Circuits and Systems II: Express Briefs, vol. 69, no. 1, pp. 65-69, 2021.
[41] Sun, Qiang, Yong-Ling Ban, Yong-Xing Che, and Zaiping Nie. "Coexistence-Mode CRLH SIW Transmission Line and Its Application for Longitudinal Miniaturized Butler Matrix and Multibeam Array Antenna." IEEE Transactions on Antennas and Propagation, vol. 69, no. 11, pp. 7593-7603, 2021.
[42] Wang, Zhan, Yuandan Dong, and Tatsuo Itoh. "Miniaturized wideband CP antenna based on metaresonator and CRLH-TLs for 5G new radio applications." IEEE Transactions on Antennas and Propagation, vol. 69, no. 1, pp. 74-83, 2020.
[43] K. Koshiji and E. Shu. "Circulators using coplanar waveguide." Electronics Letters, vol. 22, no. 19, pp. 1000-1002, 1986.
[44] B. Bayard, D. Vincent, C. R. Simovski, and G. Noyel. "Electromagnetic study of a ferrite coplanar isolator suitable for integration." IEEE Trans. Microw. Th. & Tech. vol. 51, no. 7, pp. 1809-1814, 2003.
[45] S. Joseph, R. Lebourgeois, Y. Huang, L. Roussel, and A. Schuchinsky. "Low-Loss Hexaferrite Self-Biased Microstrip and CPW Circulators." In Proc. In IEEE 2019 13rd Int. Congress on Artificial Materials for Novel Wave Phenomena (Metamaterials), pp. X-372, 2019.
[46] T. Ueda and M. Tsutsumi, "Nonreciprocal left-handed transmission characteristics of microstrip lines on ferrite substrate," IET Microwaves, Antennas and amp; Propagation, vol. 1, pp. 349-54, 2007.
[47] T. Ueda and M. Tsutsumi, "Left-handed transmission characteristics of ferrite microstrip lines without series capacitive loading," IEICE Transactions on Electronics, vol. E89-C, pp. 1318-1323, 2006.
[48] Mahmoud A. Abdalla, and Zhirun Hu. "On the study of CWP dual band left handed propagation with reciprocal and nonreciprocal characteristics over ferrite substrates." In 2007 IEEE Antennas and Propagation Society International Symposium, pp. 2578-2581, 2007.
[49] M. A. Abdalla and Z. Hu, "Nonreciprocal left handed coplanar waveguide over ferrite substrate with only shunt inductive load," Microwave and Optical Technology Letters, vol. 49, pp. 2810-2814, 2007.
[50] S. Karimian, M. Abdalla and Z. Hu, "Tunable Metamaterial Ferrite Stepped Impedance Resonator (SIR)," 2010 PIERS The 27th Progress in Electromagnetics Research Symposium, Mar. 22-26, 2010, Xi'an, China, pp 165-168.
[51] M. A. Abdalla and Z. Hu, "Compact Metamaterial Coplanar Waveguide Ferrite Tunable Resonator,"IET Microwaves, Antennas & Propagation, vol. 10, no. 4, pp. 406-412, 2016.
[52] M. A. Abdalla and Z. Hu, "Multi -band functional tunable LH impedance transformer," Journal of Electromagnetic Wave and Applications, vol. 23, pp. 39-47, 2009.
[53] M. A. Abdalla and Z. Hu, "Compact tunable left handed ferrite transformer," International Journal of Infrared and Millimeter Waves, vol.30, no. 8, pp.813-825, 2009.
[54] M. Abdalla and Z. Hu "Ferrite Tunable Metamaterial Phase Shifter", 2010 IEEE AP-S International Antenna and Propagation Symposium Digest, Toronto, Cananda, pp. 1-4, 2010.
[55] T. Ueda, K. Ninomiya, K. Yoshida, and T. Itoh. "Design of dispersion-free phase-shifting non-reciprocity in composite right/left handed metamaterials." in 2016 IEEE MTT-S Int. Microwave Symposium (IMS), pp. 1-4, 2016.
[56] T. Kodera, and C. Caloz, "Integrated Leaky-Wave Antenna–Duplexer/Diplexer Using CRLH Uniform Ferrite-Loaded Open Waveguide", IEEE Trans. Antenna and Propagation vol. 58, no. 8, pp. 2508-2514, 2010.
[57] T. Kodera, D. L. Sounas, D.L. and C. Caloz, "Tunable magnet-less non-reciprocal metamaterial (MNM) and its application to an isolator" 2012 Asia-Pacific Microwave Conference Proceedings (APMC), pp. 73-75, 2012.
[58] M. Abdalla and Z. Hu, " Compact Novel CPW Ferrite Coupled Line Circulator with Left-handed Power Divider/Combiner ", 2011 European Microwave Week, EuMW2011, Digest, Manchester, UK, pp. 794-797, October 9-14 2011.
[59] G. Sajin, S. Simion, F. Craciunoiu, A.-C. Bunea, A. Dinescu, and A. A. Muller, "Ferrite supported steerable antenna on metamaterial CRLH transmission line", 40th European Microwave Conference (EuMC), pp. 449-452, 2010.
[60] M. Abdalla and Z. Hu, " Compact and Tunable Metamaterial Antenna for Multi-band Wireless Communication applications", 2011 IEEE AP-S International Antenna and Propagation Symposium Digest, Jul. 2011, Spokane, USA, pp. 2951-2953, 2011.
[61] A. Porokhnyuk, T. Ueda, Y. Kado, Y.and T. Itoh, "Design of nonreciprocal CRLH metamaterial for non-squinting leaky-wave antenna" 2013 IEEE MTT-S International Microwave Symposium Digest (IMS), pp. 1-3, 2013.
[62] T. Kodera, D. L. Sounas, and C. Caloz, "Nonreciprocal Magnetless CRLH Leaky-Wave Antenna Based on a Ring Metamaterial Structure", IEEE Antennas and Wireless Propagation Letters, vol. 10, 2011, pp. 1551- 1554.
[63] G. Sajin, I. A. Mocanu, F. Craciunoiu, M. Carp," MM-wave left-handed transmission line antenna on anisotropic substrate" 43rd European Microwave Conference (EuMC), pp. 668-671, 2013.
[64] M. Tsutsumi, K. Okubo, "Effect of stubs on ferrite microstrip line magnetized to wave propagation", APMC 2009. Asia Pacific Microwave Conference, pp. 1234-1237, 2009.
[65] M. Tsutsumi and K. Okubo, "On the left handed ferrite coupled line," in EMTS Int. URSI Electromagnetic Theory Symposium Digest, Ottwa, Canda, pp. 1-3, 2007.
[66] M. A. Abdalla and Z. Hu, "Compact tunable single and dual mode ferrite left-handed coplanar waveguide coupled line couplers,"IET Microwaves, Antennas & Propagation, vol. 3, no. 4, pp. 695-702, 2009.
[67] M. A. Abdalla and Z. Hu, "Composite Right/Left-handed Coplanar Waveguide Ferrite Forward Coupled-Line Coupler,"IET Microwaves, Antennas & Propagation, vol. 9, no. 10, pp. 1104 –1111, 2015.
[68] M.A. Abdalla and Z. Hu, "Reconfigurable/tunable dual band/dual mode ferrite composite right/left-handed CPW coupled-line coupler",

Journal of Instrumentation, vol. 12, no. 9, pp. P09009, 2017.
[69] Abdalla, Mahmoud A., and Zhirun Hu. "Tunable characteristics of ferrite composite right/left handed coplanar waveguide coupled line coupler–Measurement and experimental verification." AEU-International Journal of Electronics and Communications, vol. 96, pp. 113-121, 2018.
[70] K. C. Gupta, R. Garg, I. bahl, and P. Bahartia, Microstrip lines and slotlines, Second ed. London: Artech House, 1996.
[71] R.K. Mongia, I. J. Bahl, P. Bhartia, and J. Hong, RF and Microwave Coupled-Line Circuits: Artech House, 2007.
[72] C. Caloz, A. Sanada, and T. Itoh, "A novel composite right-/left-handed coupled-line directional coupler with arbitrary coupling level and broad bandwidth," IEEE Transactions on Microwave Theory and Techniques, vol. 52, pp. 980-92, 2004.
[73] L. Liu, C. Caloz, C.-C. Chang, and T. Itoh, "Forward coupling phenomena between artificial left-handed transmission lines," Journal of Applied Physics, vol. 92, pp. 5560-5, 2002.
[74] Y. S. Tan, X. S. Rao, L. F. Chen, C. Y. Tan, and C. K. Ong, "Simulation, fabrication and testing of a left-handed microstrip coupler," Microwave and Optical Technology Letters, vol. 45, pp. 255-258, 2005.
[75] S.-G. Mao and M.-S. Wu, "A novel 3-dB directional coupler with broad bandwidth and compact size using composite right/left-handed coplanar waveguides," IEEE Microwave and Wireless Components Letters, vol. 17, pp. 331-3, 2007.
[76] M. Tsutsumi, "Left handed microwave ferrite circuit and devices," presented at Proceedings of the 36th European Microwave Conference, 10-15 Sept. 2006, Manchester, UK, 2006.
[77] K. Okubo and M. Tsutsumi, "On the left handed ferrite circulator," presented at 2006 IEEE MTT-S International Microwave Symposium Digest, 11-16 June 2006, San Francisco, CA, USA, 2006.
[78] M. Tsutsumi and K. Okubo, "On the left handed ferrite coupled line," presented at 2007 EMTS International URSI Commission B - Electromagnetic Theory Symposium Digest, 26-28 July 2007, Ottwa, ON, Canda, 2007.
[79] M. A. Abdalla and Z. Hu, "On the study of left-handed coplanar waveguide coupler on ferrite substrate," Progress In Electromagnetics Research Letters, vol. 1, pp. 69-75, 2008.
[80] H. Van Nguyen and C. Caloz, "Generalized coupled-mode approach of metamaterial coupled-line couplers: coupling theory, phenomenological explanation, and experimental demonstration," IEEE Transactions on Microwave Theory and Techniques, vol. 55, pp. 1029-39, 2007.
[81] Mahmoud A. Abdalla and Zhirun Hu, "A Mode Switchable Ferrite Composite Right/Left Handed Microwave Coupler", Progress In Electromagnetics Research C (PIER C), vol. 125, pp. 201-216, 2022.
[82] A. Aharoni, "Demagnetizing factors for rectangular ferromagnetic prisms," Journal of Applied Physics, vol. 83, pp. 3432-4, 1998.
[83] A. J. B. Fuller, Ferrite at microwave frequencies. Stevenage, London: Institution of Engineering and Technology, 1987.